1994

A comparison of neutron detection systems with radioisotopic neutron sources in preparation for characterization of the neutron spectra of Varian model 2100 and 2300 Clinacs®

Anna M. Johnson Teachout
San Jose State University

Order Number 1358231

A comparison of neutron detection systems with radioisotopic neutron sources in preparation for characterization of the neutron sepctra of Varian model 2100 and 2300 Clinacs®

Teachout, Anna Marie Johnson, M.S.

San Jose State University, 1994

U·M·I
300 N. Zeeb Rd.
Ann Arbor, MI 48106

A COMPARISON OF NEUTRON DETECTION SYSTEMS WITH RADIOISOTOPIC NEUTRON SOURCES IN PREPARATION FOR CHARACTERIZATION OF THE NEUTRON SPECTRA OF VARIAN MODEL 2100 AND 2300 CLINACS®

A Thesis

Presented to
The Faculty of the Department of Nuclear Science
San Jose State University

In Partial Fulfillment
of the Requirements for the Degree
Master of Science

By

Anna M. Johnson Teachout

May, 1994

APPROVED FOR THE DEPARTMENT OF
NUCLEAR SCIENCE

Dr. Peter A. J. Englert

Dr. Jeffrey H. Kleck

Dr. James C. Liu

Dr. Adrian Rodriguez

Dr. Allen Tucker

APPROVED FOR THE UNIVERSITY

Serena M. Stanford

ABSTRACT

A COMPARISON OF NEUTRON DETECTION SYSTEMS WITH RADIOISOTOPIC NEUTRON SOURCES IN PREPARATION FOR CHARACTERIZATION OF THE NEUTRON SPECTRA OF VARIAN MODEL 2100 AND 2300 CLINACS®

by Anna M. Johnson Teachout

This paper reports on a comparison of the performance of three different methods of neutron detection/spectrometry: moderated indium foil activation, the Bonner multisphere spectrometer with ^{6}LiF and ^{7}LiF thermoluminescent dosimeters, and the bubble detector spectrometer (BDS). A ^{252}Cf neutron source was used for this purpose. These data were analyzed to ascertain which method provided the "best fit" of the ^{252}Cf fission spectrum as determined by concordance with reference values. The BUNKI program was used to unfold the data from the Bonner multispheres and the BDS. Spectral stripping was also applied to the BDS data. The method given in American Association of Physicists in Medicine Report 19, National Council for Radiation Protection Report 79, and LaRiviere were used for the moderated foils. Variations in the sensitivity of the BDS were checked with a $^{238}PuBe$ radioisotopic neutron source at intervals throughout the course of the study.

Final results indicate that the Bonner multisphere system is the "better" of the three neutron detection methods, although the method is not without problems. The moderated foil method closely agreed with the reference values, but cannot provide spectral distribution data. The BDS data were subject to oscillations imposed by the non-negativity conditions in spectral stripping.

ACKNOWLEDGEMENTS

The writer would like to thank some of the people without whom this study would not have been possible. Professor Peter A.J. Englert directed my graduate studies and supplied the bubble detectors for this project. Jeffrey H. Kleck of Varian Associates, Inc. provided the Clinacs®, foil moderation detectors, support equipment and staff, along with his technical expertise and invaluable insight. James Liu and Vashek Vylet of the Radiation Health Physics Group of SLAC furnished the Bonner multispheres and TLDs, the neutron sources, the BUNKI code, a computer account at SLAC, and their commentary on interpreting the BUNKI and other data. The staff at the Dosimetry Laboratory at SLAC provided the TLD calibration equipment and readers.

TABLE OF CONTENTS

LIST OF FIGURES

Figure page

LIST OF TABLES

Chapter I

INTRODUCTION

During the early period of health physics, the lack of suitable instruments for quantitative dosimetry and spectrometry, as well as the lack of suitable units of dose, posed two of the greatest barriers to the professional development of the field. A better understanding of the interaction mechanisms and effects of radiation, coupled with technological innovations, have advanced the field such that quantitative personnel dosimetry, spectrometry, and radiation monitoring now comprise the basic precepts of health physics.

Progress has been more substantial in the development of detectors for directly ionizing radiation than for indirectly ionizing radiation such as X-rays, gamma rays, and neutrons. The detection of neutrons is difficult because neutrons carry no electric charge, and thus are not influenced by the coulombic force, which is the basis for energy transfer between electrons and charged particles. Additionally, the interaction cross-section of various types of neutrons differs markedly with neutron energy.

The most widely used methods in neutron spectrometry or dosimetry are based on the detection of the secondary charged particles resulting from an interaction of the incident neutron. Indirect neutron measurements may also be accomplished by means of neutron induced radioactivity in thin

foils. The foils are exposed to a neutron flux for a period of time and, upon removal, the induced radioactivity is counted. The measured counts can then be used to determine the total number and average energy distribution of the neutron field [1].

This study was comprised of two primary parts: a portion utilizing radioisotopic neutron sources and a portion to characterize the neutron spectra for Varian Clinacs® of differing energies (10 MV, 15 MV, 18 MV, and 20 MV). While the underlying objective of this study was the characterization of the neutron field at selected locations around the medical accelerators, the research conducted with the radioisotopic neutron sources was a pre-requisite to that objective.

The three methods employed in both portions of this study were moderated foil activation, the Bonner multisphere spectrometer, and the bubble detector spectrometer. Two radioisotopic neutron sources were utilized in this study toward different ends: ^{238}PuBe and ^{252}Cf. The PuBe source was used to check the sensitivity of the bubble detector spectrometer throughout the duration of the research (~6 months). The ^{252}Cf source was used to compare and contrast the performance of each of the three detection methods employed in this study. The results of this comparison were then analyzed to determine which of the three methods provided the "best fit" of the fission spectrum as determined by concordance with

reference values for the fission source (e.g., the neutron fluence, average energy, and dose equivalent). The resulting "best" method was then used as a reference or "benchmark" in characterizing the neutron spectra for the four Clinacs®. Although this author fully participated in all aspects of the setup and research for both portions (radioisotopic and accelerator) of this study, it was necessary for dissertation submission purposes to divide the study between this author and a fellow researcher (Elsalim) on the project. Hence the focus of this dissertation will be on the radioisotopic portion of the study, and the accelerator portion will be addressed in a separate publication and dissertation.

Prior to discussing the experimental method, the underlying principles of operation of each of these methods is presented. Compared to the moderated foils and multisphere spectrometer methods, the bubble detector spectrometer is a relative "newcomer" and as such its properties may not be as well known. For this reason, a more detailed background is presented for the bubble detector spectrometer than for that of the other two methods.

BIBLIOGRAPHY

[1] American Association of Physicists in Medicine, "Neutron Measurements around High Energy X-Ray Radiotherapy Machines," AAPM Report Number 19 (1986).

Chapter II

NEUTRON DETECTION WITH SUPERHEATED LIQUIDS

2.1 INTRODUCTION

One of the earliest uses of superheated liquids in radiation detection was the bubble chamber, invented by Glaser in 1952 [1]. During the peak period for bubble chamber physics (1955-1975), every major accelerator operated at least one [2]. Although bubble chambers have seen occasional use in neutron spectrometry [3], they were not generally considered practical for use in health physics applications because of their size, complexity, and operating expense. Contemporary bubble detectors operate on the same principle as the bubble chamber, that is, radiation interactions create secondary charged particles which deposit energy along their path and initiate vapor bubble formation (boiling) in superheated liquids.

Bubble detectors are available commercially from Apfel (Apfel Enterprises, Inc., 25 Science Park, New Haven, CT 06511) and Chalk River Nuclear Laboratory (Bubble Technology Industries, Inc., Hwy. 17, Chalk River, Ontario, Canada KOJ 1JO). Apfel manufactures the Superheated Drop Detector (SDD)™ [4], which consists of a number (30,000 - 40,000) of superheated droplets of CF_2Cl_2 suspended in a semi-solid matrix of water, glycerine, and gel. Bubble Technology Industries, Inc. (BTI) produces the Bubble-Damage Polymer Detector, or

Bubble Detector (BD), which utilizes a similar amount of microscopic superheated drops dispersed throughout a firm polymer [5].

2.2 THEORY OF BUBBLE NUCLEATION

Even though the absolute mechanism of vapor bubble nucleation is not fully understood, it is generally agreed that the thermal spike model of Seitz offers an appropriate explanation [6]. According to this theory, intense ionization and excitation along the charged particle's path produces localized heating or hot spots, which explode, causing minute vapor bubbles to develop. When a bubble reaches a thermodynamically unstable size (defined by the critical radius, R_c), it will grow to a visible size via liquid-to-vapor transformation (evaporation) of the superheated liquid until the entire droplet is consumed. The critical radius is given by

$$R_c = 2\gamma(T)/\Delta P$$

where $\gamma(T)$ is the surface tension at temperature T and $\Delta P = P_v(T) + P_g - P_o$, with P_v being the pressure of the vapor in the container, P_g the partial pressure associated with non-condensible dissolved gas, and P_o the externally applied pressure [7]. ΔP is a measure of the degree of the liquid's superheat, and as ΔP increases R_c becomes smaller and the energy needed for vaporization of the drop also decreases.

2.3 NEUTRON SPECTROMETRY WITH BUBBLE DETECTORS

Bubble Technology Industries (BTI) offers neutron spectroscopy with their bubble detector spectrometer (BDS) package. By capitalizing on the fact that the neutron energy threshold of bubble formation depends on the degree of superheat of the detector liquid, BTI can selectively prepare detectors with varying neutron energy thresholds [8].

2.4 PROPERTIES OF THE BUBBLE DETECTOR SPECTROMETER

Bubble detectors such as the BDS are primarily produced and used in small, sealed test tubes, as shown in Figure 2.1 [9]. The detectors are originally pressurized to 5 atm, and a small amount of volatile liquid floats on the polymer medium to maintain this pressure. In this pressurized state, the detector is unresponsive to radiation. Prior to exposure, the screw top is loosened to release the pressure. This causes

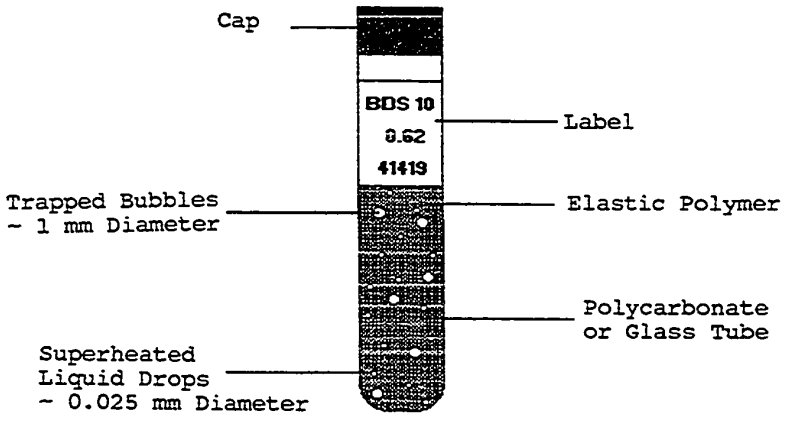

Figure 2.1. Illustration of the bubble detector. Dimensions of the active volume are 1.6 cm diameter by 8 cm height.

the liquid droplets to superheat, thereby activating the detector. Neutron irradiation interactions cause droplet vaporization and formation of visible gas bubbles that are trapped at their formation site by the polymer medium. The bubbles are then counted, either by manual counting (as was the case in this study), or with the aid of the Bubble Technology BDR-Series II automatic reader. According to the manufacturer, the BDS features the following properties:

1. Neutron spectrometry from 10 keV to 20 MeV $\pm$ 10% for most neutron fields. Six different fixed energy thresholds.
2. Readings immediate upon exposure.
3. Reusable. A recompression chamber is available for resetting the detectors.
4. Isotropic response.
5. Dose range from less than 10 μSv to over 1 mSv.
6. Sensitivity from approximately 0.5 to 5 bubbles/mrem; higher sensitivities for some thresholds are available upon request.
7. Gamma radiation discrimination.
8. Not effected by humidity.
9. Useable at room temperatures (20 °C).

2.5 EXPERIMENTAL SETUP - BDS

The BDS utilized in this study consisted of 36 bubble detectors which provided neutron energy thresholds at

approximately 10 keV, 100 keV, 600 keV, 1 MeV, 2.5 MeV and 10 MeV (six detectors for each of the six different energy thresholds). The detectors were identified as BDS-10, BDS-100, et cetera, with the number referencing the energy threshold of the bubble detector spectrometer in units of keV. Depending on the quality of spectral data needed and the measurement circumstances, the detectors may be used in one of several combinations, e.g., six detectors, one from each of the six energy thresholds; three detectors of each of six energy thresholds; or three or six detectors from identical energy thresholds [10]. The combination of six detectors from identical energy thresholds was used in this study to improve counting statistics.

The detectors in our spectrometer set were serial numbered 41415 through 41450, and were calibrated by BTI at 20°C with an accuracy of $\pm$ 10% using an AmBe neutron source. The sensitivity values supplied with each detector were based on the dose equivalent as defined in the National Council on Radiation Protection and Measurements Report Number 38, *Protection against Neutron Radiation*. Figure 2.2 shows the normalized measured response functions for the six different thresholds in the standard BDS set [10]. The response function values are in bubbles per unit incident fluence on the detectors for detectors having a sensitivity of unity.

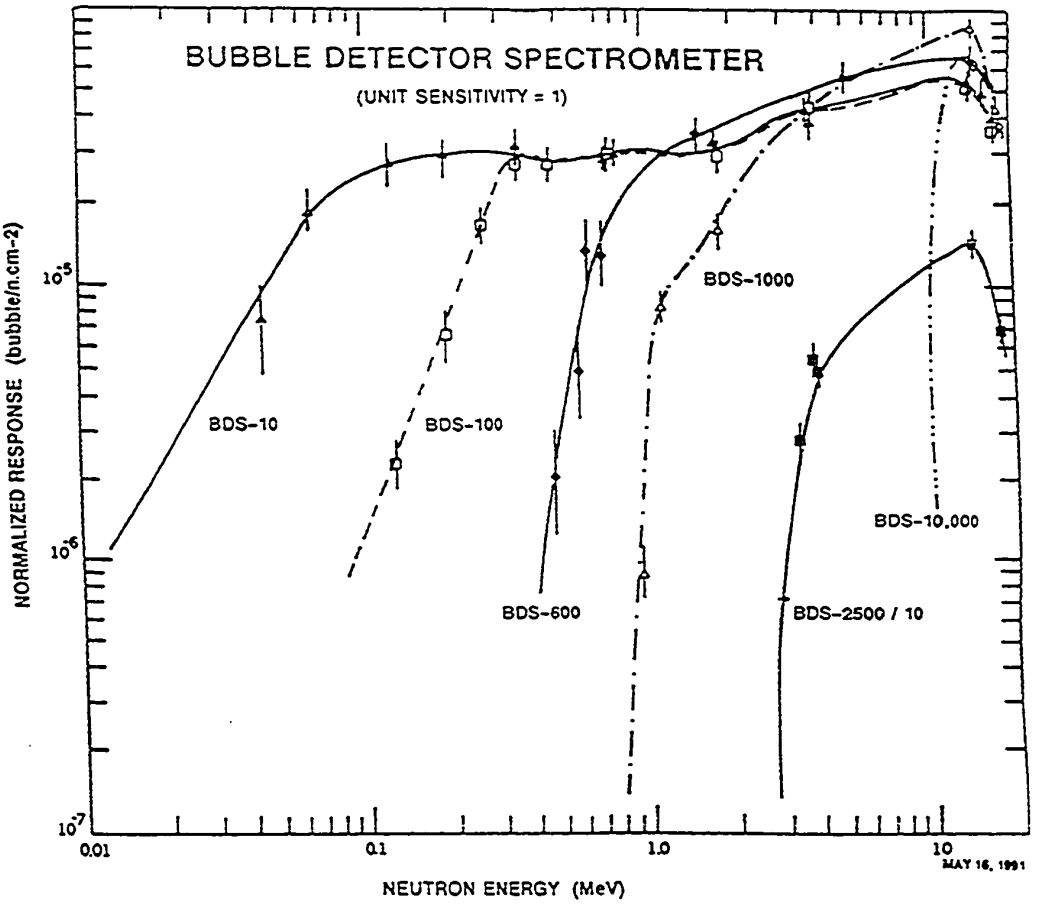

Figure 2.2. The normalized measured response functions for the six energy thresholds of the Bubble Detector Spectrometer. (From Reference 10.)

BIBLIOGRAPHY

[1] H. Ing and H.C. Birnboim, "A bubble-damage polymer detector for neutrons," Nucl. Tracks Radiat. Meas. 8(1-4), 285-288 (1984).

[2] I.S. Hughes, Elementary Particle Physics, 3rd ed. (Cambridge, Cambridge, 1991), p. 20.

[3] H.E. Adelson, H.A. Bostick, B.J. Moyer and C.N. Waddell, "Use of the four-inch liquid hydrogen bubble chamber as a fast-neutron spectrometer," Rev. Sci. Instr. 31(1), 1-10 (1960).

[4] R.E. Apfel, Detector and dosimeter for neutrons and other radiation, U.S. pat. 4,143,274 (1979).

[5] H. Ing, "The status of the bubble-damage polymer detector," Nucl. Tracks Radiat. Meas. 12, 49-54 (1986).

[6] F. Seitz, "On the theory of the bubble chamber," Phys. Fluids 1, 2-13 (1958).

[7] R.A. Apfel, "The superheated drop detector," Nucl. Inst. and Meth. 162, 603-608 (1979).

[8] H. Ing and K. Tremblay, "To Develop a Set of Variable Lower-Energy Threshold Bubble Neutron Detectors for Use as a Spectrometer," Final Report on contract W7714-7-5263/01-SV for DREO, BTI-88/2-29A, 29 February 1988.

[9] H. Ing, "The status of the bubble-damage polymer detector," Nucl. Tracks Radiat. Meas. 12, 49-54 (1986).

[10] Bubble Technology Industries "Instruction Manual for the Bubble Detector Spectrometer (BDS)," BTI, Inc., January 31, 1992.

Chapter III

MULTISPHERE TECHNIQUES

3.1 INTRODUCTION

In 1960, Bramblett et al. [1] investigated a new type of neutron spectrometer which employed a small (4 mm high, 4 mm diameter) ^{6}LiI(Eu) scintillator placed at the center of polyethylene moderating spheres ranging in size from 2 to 12 inches in diameter. Varying the diameter of the moderator results in different energy response characteristics for the respective detector. The behavior seen in this type of study is shown in Figure 3.1 [2]. Bonner was the senior author of the original paper, hence such spheres have become known as "Bonner Spheres," and are also widely referred to as Bonner multispheres, or simply multispheres.

Bonner spheres are used in conjunction with various types of thermal neutron detectors. In addition to the ^{6}LiI(Eu) scintillator, multisphere experiments have been conducted with BF_3 or ^{3}He proportional counters, indium or gold activation foils, and ^{6}LiF-^{7}LiF thermoluminescent dosimeter pairs [3].

3.2 POTENTIAL DRAWBACKS OF THE MULTISPHERE METHOD

Although the multisphere method has seen widespread application in neutron spectrometry, it is not without drawbacks. As indicated in Figure 3.1, the response functions are rather broad, consequently the method tends to be of poor

energy resolution. Accurate knowledge of the response functions and access to an appropriate mathematical method for unfolding the neutron spectrum are necessary to successfully utilize the multisphere technique. Detector response functions have not been determined experimentally over the entire energy range of many neutron spectra for which the technique is used, resulting in dependence upon theoretically generated response functions [3]. Subsequently, disagreements are common between a given differential test spectrum and the one synthesized from calculated responses [4]. Stevenson [5] has shown that introduction of errors in the response

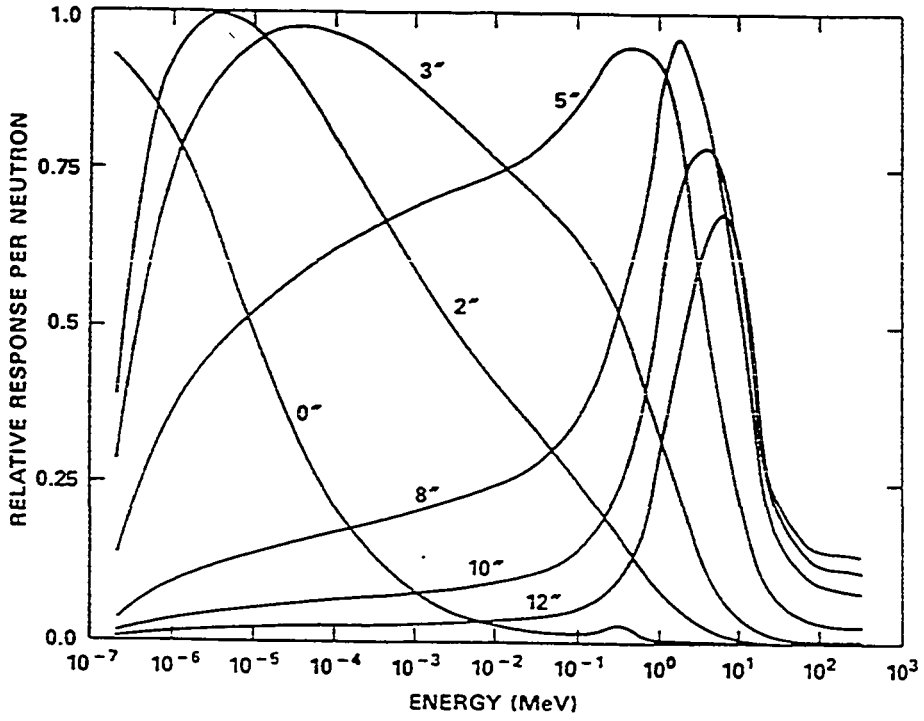

Figure 3.1. The energy dependence of the relative detection efficiencies of Bonner sphere neutron detectors of various diameters up to 12 inches. (From Knoll, Reference 2.)

functions enhances these discrepancies. However, careful experimental technique and critical use of unfolding codes can yield acceptable agreement in the computed values of integrated quantities such as fluence and dose.

When choosing an unfolding method for a specific application, it is prudent to select a program which has been successfully applied in comparable applications, or, if possible, to solicit the advice of an expert in the use of unfolding codes [6] . The selection process is facilitated by a number of reviews and intercomparisons [7][8][9].

3.3 EXPERIMENTAL SETUP - MULTISPHERE SPECTROMETER

In this study, multispheres of 2, 3, 5, 8, 10, and 12 inch diameters were used with two pair of Teledyne ^{6}LiF-^{7}LiF thermoluminescent dosimeters (TLDs) per sphere. The program BUNKI was utilized to unfold the neutron spectra from data acquired as a result of exposure of the multispheres and BDS detector systems to a ^{252}Cf neutron source. A description of BUNKI is provided in Appendix A, and a characterization of the ^{252}Cf source is given by Hertel and McDonald [10] and Liu et al. [11]. Because data was not available on the response matrix of the TLDs used, trials were run with numerous response matrices to determine which provided the "best" fit of the ^{252}Cf spectrum. The SAN13 [12] response matrix (12.7 mm X 12.7 mm ^{6}LiF detector) was chosen on the basis of these comparisons. The calculated values for the

SAN13 response matrix are given in Table 3.1.

TABLE 3.1

Multisphere Spectrometer SAN13 Response Matrix

Weighted P_6 Calculation[a]

Moderator = CH_2 (density = 0.95 g/cm^2) Detector = 12.7 mm X 12.7 mm ^{6}LiI

Group No.	Sphere Diameter (inches)					
	2	3	5	8	10	12
1	2.6688E−03	9.4522E−03	5.3670E−02	1.5952E−01	2.2323E−01	2.7362E−01
2	2.1231E−03	9.7606E−03	5.8571E−02	1.7132E−01	2.3598E−01	2.8445E−01
3	2.0391E−03	1.0949E−02	6.5482E−02	1.8362E−01	2.4616E−01	2.8902E−01
4	2.3485E−03	1.3631E−02	8.1165E−02	2.1967E−01	2.8638E−01	3.2629E−01
5	3.4051E−03	2.0081E−02	1.1728E−01	3.0445E−01	3.8448E−01	4.2313E−01
6	5.8470E−03	3.3881E−02	1.9211E−01	4.7422E−01	5.7736E−01	6.1121E−01
7	1.2072E−02	7.0499E−02	3.9990E−01	9.6063E−01	1.1375E+00	1.1651E+00
8	2.9253E−02	1.5962E−01	7.6720E−01	1.4814E+00	1.5282E+00	1.3649E+00
9	6.3695E−02	3.1635E−01	1.2342E+00	1.8081E+00	1.5588E+00	1.1594E+00
10	1.2832E−01	5.6562E−01	1.7510E+00	1.8966E+00	1.3377E+00	8.0866E−01
11	2.1645E−01	8.0115E−01	1.8795E+00	1.4309E+00	7.9897E−01	3.8047E−01
12	3.3594E−01	1.0376E+00	1.9029E+00	1.0796E+00	5.0540E−01	2.0510E−01
13	4.3882E−01	1.2026E+00	1.8033E+00	8.2364E−01	3.4749E−01	1.3101E−01
14	5.4548E−01	1.3172E+00	1.6825E+00	6.6755E−01	2.6804E−01	9.8550E−02
15	6.5065E−01	1.4065E+00	1.5885E+00	5.7621E−01	2.2598E−01	8.2343E−02
16	7.5335E−01	1.4868E+00	1.5274E+00	5.2913E−01	2.0216E−01	7.3375E−02
17	8.5970E−01	1.5663E+00	1.4954E+00	4.8514E−01	1.8640E−01	6.7504E−02
18	9.7310E−01	1.6455E+00	1.4517E+00	4.5667E−01	1.7444E−01	6.3074E−02
19	1.0949E+00	1.7225E+00	1.4191E+00	4.3205E−01	1.6429E−01	5.9333E−02
20	1.2246E+00	1.7944E+00	1.3838E+00	4.0917E−01	1.5504E−01	5.5938E−02
21	1.3605E+00	1.8580E+00	1.3438E+00	3.8706E−01	1.4625E−01	5.2729E−02
22	1.4992E+00	1.9092E+00	1.2972E+00	3.6504E−01	1.3763E−01	4.9594E−02
23	1.6365E+00	1.9446E+00	1.2440E+00	3.4308E−01	1.2915E−01	4.6514E−02
24	1.7659E+00	1.9600E+00	1.1840E+00	3.2098E−01	2.2070E−01	4.3455E−02
25	1.3782E+00	1.9498E+00	1.1161E+00	2.9833E−01	1.1211E−01	4.0350E−02
26	1.9620E+00	1.9081E+00	1.0391E+00	4.7472E−01	1.0321E−01	3.7135E−02
27	2.0018E+00	1.8265E+00	9.5107E−01	2.4943E−01	9.3078E−02	3.3709E−02
28	1.9766E+00	1.6934E+00	8.4815E−01	2.2133E−01	8.3184E−02	2.9920E−02
29	1.8534E+00	1.4906E+00	7.2353E−01	1.8852E−01	7.0913E−02	2.5509E−02
30	1.6342E+00	1.2380E+00	5.8863E−01	1.5371E−01	5.7914E−02	2.0844E−02
31	7.8070E−01	5.6810E−01	2.7270E−01	7.2292E−02	2.7389E−02	9.8840E−03

[a] R.S. Sanna, "Thirty One Group Response Matrices for the Multisphere Neutron Spectrometer over the Energy Range Thermal to 400 MeV," Atomic Energy Commission Report No. HASL−267 (1973).

BIBLIOGRAPHY

[1] R.L. Bramblett, R.J. Ewing, and T.W. Bonner, "A New Type of Neutron Spectrometer," Nucl. Inst. Meth., 9, 1 (1960).

[2] G.F. Knoll, Radiation Detection and Measurement, 2d ed., John Wiley and Sons, p. 517 (1989).

[3] R.H. Thomas and G.R. Stevenson, "Radiation Protection Around High Energy Accelerators," Radiat. Prot. Dosim. 10, 283 (1985).

[4] H.W. Patterson and R.H. Thomas, Accelerator Health Physics, Academic Press, p. 260 (1973).

[5] G. Stevenson, Neutron Spectrometry from 0.025 eV to 25 GeV, Rutherford High-Energy Laboratory report RHEL/R154, Nov. 1967.

[6] N.E. Hertel, Georgia Institute of Technology, 1993 (private communication).

[7] J.T. Routti and J.V. Sandberg, "Unfolding Activation and Multisphere Detector Data," Radiat. Prot. Dosim. 10, 107 (1985).

[8] N.E. Hertel and J.W. Davidson, "The Response of Bonner Spheres to Neutrons from Thermal Energies to 17.3 MeV," Nucl. Instr. Meth. Phys. Res. A, 238, 509 (1985).

[9] T.L. Johnson, Y. Lee, K.A. Lowry and S.G. Gorbics, "Recent Advances in Bonner Sphere Neutron Spectrometry," in American Nuclear Society Proceedings on Theory and Practices in Radiation Protection and Shielding, ANS, ISBN:0-89448-132-0 (1987).

[10] N.E. Hertel and J.C. McDonald, "Calculations of Anisotropy Factors and Dose Equivalents for Unmoderated ^{252}Cf Sources," Radiat. Prot. Dosim. 32, pp. 77-82 (1990).

[11] J.C. Liu, T.M. Jenkins, R.C. McCall, and N.E. Ipe, "Neutron Dosimetry at SLAC: Neutron Sources and Instrumentation," Stanford Linear Accelerator Center Publication No. SLAC-TN-91-3 (1991).

[12] R.S. Sanna, "Thirty One Group Response Matrices for the Multisphere Neutron Spectrometer over the Energy Ranges Thermal to 400 MeV," Atomic Energy Commission report no. HASL-267 (1973).

Chapter IV

NEUTRON DETECTION BY ACTIVATION

4.1 INTRODUCTION

Activation detectors operate on the principle of the transformation of stable nuclei into radioactive species by bombardment with particulate radiation, or by photon radiation possessing sufficient energy for photonuclear reactions. Thermal and slow neutrons are effective in this regard as neutron reaction cross sections are greatest at low neutron energies. Typical reactions which produce specific radionuclides may be found in the literature [1][2].

Moderating materials are commonly used in conjunction with metal foils as neutron activation detectors. A thin foil within a moderator is exposed to a neutron flux for a recorded period of time. At the end of the irradiation, the foil is removed from the moderator and the induced radioactivity in the foil is counted, with the decay and counting times recorded. The moderator may consist of paraffin, water, polyethylene, cadmium-paraffin, boron-paraffin or other similar combinations. The moderator provides an energy independent thermal neutron flux at the foil which is proportional to the incident fast neutron flux for energies up to several MeV.

Neutron activation detectors have many advantages [3]:

a. Numerous simultaneous measurements are possible, and

the locations where foils may be placed are unrestricted.

c. The results are unambiguous, as the induced activity is caused solely by neutrons.

d. Foils are not disabled by high neutron flux rates.

e. They respond correctly in pulsed radiation fields.

The most widely used activation foils are gold and indium, both of which have advantages and disadvantages that are well documented in the literature [4][5].

4.2 EXPERIMENTAL SETUP - MODERATED FOIL METHOD

Indium was used as the activation foil for this study. The nuclear reactions for its activation and decay are

$$^{115}_{49}In + ^{1}_{0}n \rightarrow ^{116}_{49}In \qquad (1)$$

and

$$^{116}_{49}In \rightarrow \beta^{-} + ^{116}_{50}Sn. \qquad (2)$$

^{116}In has a half-life $t_{\frac{1}{2}}$ = 54.15 minutes [6].

Two types of moderators were utilized with the indium foils: flux integrators fabricated by McCall [7] to determine the fluence, and an Andersson-Braun remmeter to determine the neutron dose equivalent. The flux integrators were borosilicate sheathed cylinders of low-density polyethylene 15.24 cm diameter by 15.24 cm length housed in an outer cover of ABS plastic ~ 0.5 cm thick. McCall estimated the response of the flux integrators to be flat within ± 30%, up to approximately 3-4 MeV [8]. The BF_3 tube and corresponding electronics were removed from the remmeter based

on the previous findings of Rogers [9], and a polyethylene plug with a slitted end to hold the indium foil near the cavity center was substituted. With a BF_3 tube as the detector, Andersson and Braun described the energy response of their remmeter as uniform from thermal neutron energies upwards to 10 MeV [10]. Figure 4.1 illustrates the energy dependence of the Anderson-Braun remmeter [11].

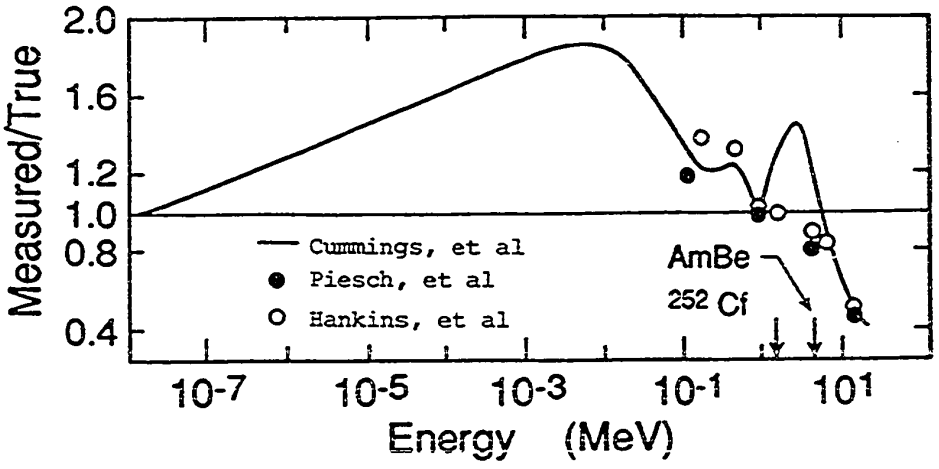

Figure 4.1 Energy dependence of the Andersson-Braun remmeter. (From SLAC-TN-91-3, Reference 11).

BIBLIOGRAPHY

[1] E. Browne and R.B. Firestone, Table of Radioactive Isotopes, John Wiley and Sons (1986).

[2] W. Lederer and V. Shirley, Table of Isotopes, John Wiley and Sons (1979).

[3] A.J. Miller and L.D. Stephens "Moderated Indium Foils," Laboratory Manual to accompany Accelerator Health Physics, Academic Press, p. 609 (1973).

[4] American Association of Physicists in Medicine "Neutron Measurements around High Energy X-Ray Radiotherapy Machines," Report No. 19 (1986).

[5] G.F. Knoll, Radiation Detection and Measurement, 2d ed., John Wiley and Sons, pp. 705-707 (1989).

[6] E. Browne and R.B. Firestone, Table of Radioactive Isotopes, John Wiley and Sons, p. 116-2 (1986).

[7] McCall Associates, 170 Hobart Heights, Woodside, CA 94062.

[8] R.C. McCall, SLAC, 1993 (private communication).

[9] D.W.O. Rogers, "Why Not to Trust a Neutron Remmeter," Health Phys. 37, 735 (1979).

[10] I.O. Andersson and J. Braun, "A Neutron Rem Counter With Uniform Sensitivity from 0.025 eV to 10 MeV," in *Neutron Dosimetry*, IAEA, Vienna (1963).

[11] J.C. Liu, T.M. Jenkins, R.C. McCall, and N.E. Ipe, "Neutron Dosimetry at SLAC: Neutron Sources and Instrumentation," Stanford Linear Accelerator Center Publication No. SLAC-TN-91-3 (1991).

Chapter V

SENSITIVITY CHECK OF THE BUBBLE DETECTOR SPECTROMETER

5.1 PURPOSE OF SENSITIVITY CHECK

Bubble Technology Industries, Inc. (BTI) specifies a post-use storage period for their neutron bubble detector spectrometer (BDS) of up to three months in a refrigerator (6°C), with bubbles recompressed as they appear [1]. In effect, this time period is the manufacturer's "warranty" that the response (sensitivity) of the BDS should remain reasonably stable for 90 days after activation (within ± 10 percent), based on extensive tests of the BDS at BTI.[1]

As it was anticipated that the entire scope of this study would likely extend beyond the "warranty" period, and because the sensitivity of the BDS is known to vary over time, it was determined that some provision should be made to periodically check the sensitivity of the bubble detector spectrometer.

5.2 SOURCE USED FOR THE SENSITIVITY CHECK OF THE BDS

The neutron source utilized for all sensitivity checks was a ^{238}PuBe radioisotopic neutron source, designated MRC-426 (for Monsanto Research Corporation, the original

[1] There were, however, two cases cited by R. Noulty of BTI of separate research efforts at Atomic Energy of Canada (using the BD-100R) and the U.S. Naval Academy (using the BDS) in which the bubble detectors were utilized in excess of six months, with only a slight decrease in detector sensitivity.

manufacturer). The MRC-426 PuBe source is composed of a metallic alloy of plutonium and beryllium cylindrically encapsulated in an inner tantalum housing and an outer stainless steel container. The isotopic percentages of the source at the time of manufacture were: 78.2% ^{238}Pu, 20% ^{239}Pu, 1.6% ^{240}Pu, and 0.2% ^{241}Pu [2]. The MRC-426 source was calibrated by the manufacturer against a National Institute of Standards and Technology (NIST) calibrated ^{238}PuBe source [3]. Table 5.1 provides the dosimetric parameters of the ^{238}PuBe source calculated for the sensitivity check of 5 February 1993. Corrections to the neutron emission rate for the ingrowth of ^{241}Am are not presented in Table 5.1. Calculations for the later sensitivity checks are given in Appendix B. The uncertainty value stated in Table 5.1 for the neutron emission rate was provided in reference 2.

5.3 EXPERIMENTAL SETUP AND PROCEDURE

The activation and first sensitivity check (irradiation) of the BDS with the ^{238}PuBe source occurred on December 31, 1992, in Building 003, the Stanford Linear Accelerator Center, Palo Alto, California. Subsequent sensitivity checks with the same PuBe source occurred in the same location on 5 February 1993, 11 March 1993, 2 June 1993 and 3 June 1993.[2]

---

[2] The data from the 31 December 1992 check will not be included for the following reasons: 1) The water bath was not used. 2) The room temperature varied from about 18-20 °C during the course of the exposure and the thermometer used on that date (approximately 6 cm in length) was

The spectrometer set was originally calibrated at 20°C and the change in detector energy response with temperature has not been fully characterized [1], therefore the bubble detectors were cooled by means of a water bath to 20°C for 30 to 45 minutes prior to commencing irradiation (with the exception of the irradiation of 31 December 1992). Additionally, efforts were made to keep the temperature of the room at or very near 20°C for the duration of the irradiation. This was accomplished by measuring the temperature at the irradiation location with a mercury-filled glass thermometer[3] and adjusting conditions accordingly, e.g., increasing or reducing the thermostat setting, opening the building doors, setting up fans. To further insure that the detectors remained at 20°C, two receptacles were fashioned from a portion of the original styrofoam shipping carton to hold six detectors each. The carton was cut so that seven wells were in a row, then the fourth (middle) well was totally drilled through to enable a pole to be inserted to hold the receptacle in place during exposure. The dimensions of the styrofoam receptacle were 19.7 cm length by 8.6 cm depth. The wells were 1.91 cm in diameter, spaced 2.54 cm apart. The distance

---

inadequate for accurate temperature measurement. 3) The setup consisted of six detectors held in place between a foam yoke with duct tape. The detectors' weight eventually led to "sagging" in the tape, hence the detectors did not remain in a uniform configuration during irradiation.

[3] Brooklyn P-M Thermo Co. 65305, 85 mm immersion, 305 mm total length, temperature range -10° to 110°C.

TABLE 5.1

Characteristics of the Radioisotopic ^{238}PuBe Neutron Source

Average Energy [MeV]	4.2	
Half-life [yr]	87.74	
Neutron Emission Rate [s^{-1}]		
as of 1 May 1990[a]	1.84×10^7	± 10%
on 5 February 1993	1.80×10^7	± 10%
Anisotropic Factor[a]	1.09	
ϕ_d[b] [cm^{-2} s^{-1}] at 0.5 m on 5 February 1993	625	
ϕ_s/ϕ_d[c] at 0.5 m 5 February 1993	2.61%	
ϕ[d] [cm^{-2} s^{-1}] at 0.5 m on 5 February 1993	640.9	
H_d[e] [mrem h^{-1}] at 0.5 m		
on 1 May 1990[a]	83.8	
on 5 February 1993	81.99	
H_s/H_d[f] at 0.5 m 5 February 1993	0.97%	
H[g] [mrem h^{-1}] at 0.5 m		
on 1 May 1990[a]	85.5	
on 5 February 1993	82.78	

[a] From SLAC-TN-91-3, October 1991.
[b] Direct fluence rate $\phi_d = NF/4\pi r^2$, where N = neutron emission rate, F = anisotropic factor, and r is the detector-to-source distance in cm.
[c] Scattered/direct fluence ratio (ϕ_s/ϕ_d) is estimated from R.B. Schwartz and C.M. Eisenhauer, "Procedures for Calibrating Neutron Personnel Dosimeters," NBS Special Publication 633 (1982). The height for both the detector and source in centimeters was 157.77.
[d] Total fluence rate $\phi = \phi_d + \phi_s$.
[e] Direct dose equivalent rate $H_d = \phi_d h_\phi$, where h_ϕ is the fluence-to-dose equivalent conversion factor. For reference, see note a.
[f] Scattered/direct dose equivalent ratio (H_s/H_d). Same derivation method as note c.
[g] Total dose equivalent rate $H = H_d + H_s$.

from the front face of the receptacle to the front edge of the well holes was 0.8 cm (this thickness was determined to be insignificant); the distance from the rear face of the receptacle to the rear edge of the well holes was 1.4 cm. A top and side view of one of the styrofoam receptacles is shown in Figure 5.1.

For the 5 February irradiation, the ^{238}PuBe source was placed on top of a square styrofoam pillar. The remaining irradiations of 11 March, 2 June, and 3 June 1993 utilized an inverted "L" type, adjustable-height pole to hold the ^{238}PuBe source in place during irradiation. The latter setup is shown in Figure 5.2. The source-to-detector distance (center of source to axis through the center of the active volume of detectors) was 50 cm for all of the irradiations. The heights for both the source and detectors in centimeters are given in Table 5.1 (5 February) or in Appendix B (all other checks).

Preliminary calculations were conducted prior to each irradiation to approximate the time required to produce an average minimum of 60-70 bubbles per detector per group based on the ^{238}PuBe source emission rate and the sensitivity values (bubbles/mrem) provided by BTI. An example of these calculations is provided in Appendix B. For good statistics, BTI recommends about 100 bubbles per detector, however, it was discovered that manual counting of more than 60-70 bubbles is extremely difficult and subject to inaccuracies, thus irradiation times were adjusted such that an average of 70-80

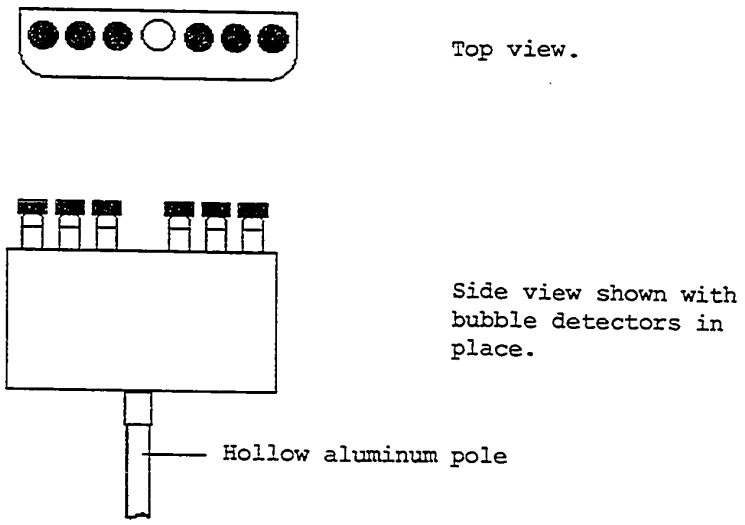

Figure 5.1. Top and side views of the styrofoam receptacle used to hold the bubble detectors during irradiation.

bubbles were obtained per group, with the exception of the BDS 10000s. There are very few neutrons at or above 10 MeV in a ^{238}PuBe source, hence even long irradiation times (> 5000 seconds) yielded an average number of bubbles much lower (on the order of 10-15 bubbles) than those of the other energy groups.

A portable "light table" was used to illuminate the irradiated detectors for bubble counting. Each detector in each group was counted four times, twice by the author and twice by the co-researcher of this study. The four counts per detector were averaged, then the averaged values from the six detectors in each group were averaged to obtain the number of bubbles per group to be used in the data analysis.

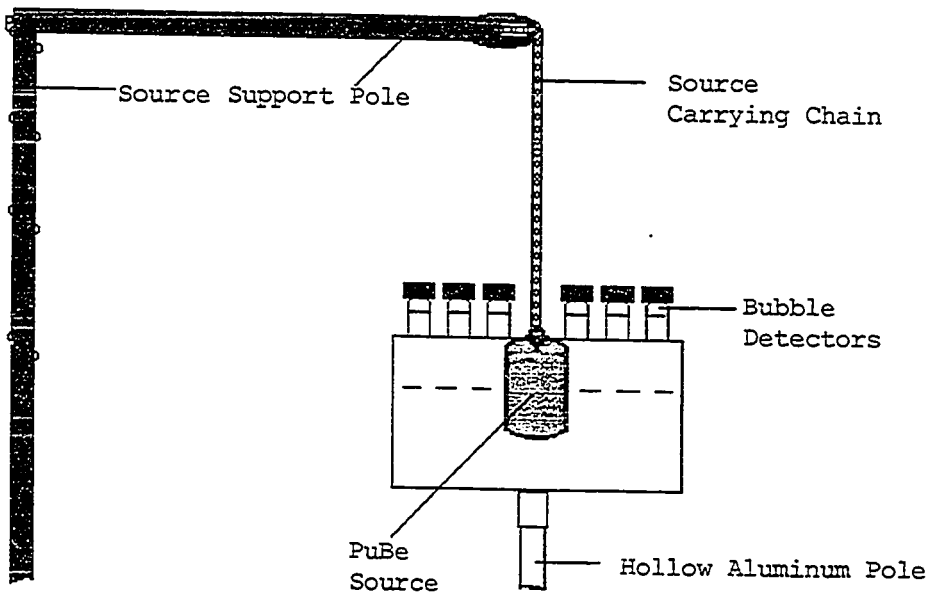

Figure 5.2. The ^{238}PuBe experimental setup (side view). The shaded items (source and source support pole) are in the foreground, and the unshaded items (bubble detectors, receptacle and aluminum pole) are 50 cm in the background.

BIBLIOGRAPHY

[1] Bubble Technology Industries "Instruction Manual for the Bubble Detector Spectrometer (BDS)," BTI, Inc., January 31, 1992.

[2] "The Source Reference Book," Stanford Linear Accelerator Radiation Physics Group (1988).

[3] J.C. Liu, T.M. Jenkins, R.C. McCall, and N.E. Ipe, "Neutron Dosimetry at SLAC: Neutron Sources and Instrumentation," Stanford Linear Accelerator Center Publication No. SLAC-TN-91-3 (1991).

Chapter VI

EXPERIMENTAL SETUP AND CALIBRATION WITH ^{252}CF

6.1 PURPOSE OF CALIBRATION

Fission neutron source spectra, particularly that of ^{252}Cf, are well known and extensively covered in the literature [1][2][3]. Therefore, ^{252}Cf was considered the logical choice for comparing the performance of the three neutron detection methods employed in this study. This comparison was used to determine which of the three methods provided the most accurate spectral information or "best fit" against reference values for average energy, fluence, and dose equivalent, and was subsequently used as a "benchmark" for the medical linear accelerator portion of this study at Varian Associates, Inc. The radioisotopic source comparison of the three detection systems' responses and the procedure followed to "benchmark" the best fit spectra are addressed in this paper.

6.2 CALIFORNIUM-252 SOURCE USED FOR THE CALIBRATION

The ^{252}Cf neutron source used in this study was a Savannah River encapsulated cylinder mounted onto the end of an aluminum rod for carrying and/or storage purposes. Overall dimensions of the rod were 296.5 cm length by 2.5 cm diameter. The original documentation providing the exact dimensions of the source encapsulation was not available; however, the encapsulation housing was estimated to be approximately 8 cm

in length by 2.5 cm in diameter. The source is stored outdoors in a shielded enclosure at the low-level storage facility at SLAC. The source had been calibrated by the Savannah River Laboratory against a NIST-calibrated ^{252}Cf source [4]. The dosimetric parameters of the ^{252}Cf source are provided in Table 6.1.

6.3 EXPERIMENTAL SETUP AND PROCEDURE

The irradiation of the multisphere/TLD detectors with the ^{252}Cf neutron source took place on March 24 and 25, 1993. Due to inclement weather (rain) and because the experiment was conducted outdoors, the BDS irradiation was postponed until April 7, 1993. The flux integrator and rem meter irradiations were conducted on April 8, 1993. To reduce exposure times and minimize detector scattering effects, a source-to-detector distance of 75 cm was chosen for all detection systems. Ground scattering effects were minimized by mounting the source and detectors 226.5 cm above the ground. Front and side views of the experimental setup are shown in Figures 6.1 and 6.2. Figures 6.1 and 6.2 are not drawn to scale, but serve for illustrative purposes.

Preliminary calculations of exposure times based on the values in Table 6.1 were conducted prior to irradiation. Each of the multispheres, the flux integrator, and remmeter were separately irradiated for one hour. The irradiation times for the BDS (cooled to 20°C with the water bath) varied from 2 to

TABLE 6.1

Characteristics of the ^{252}Cf Spontaneous Fission Neutron Source

Average Energy [MeV]	2.07	
Half-life [yr]	2.645	
Neutron Emission Rate [s^{-1}]		
as of 1 May 1990[a]	4.92×10^8	± 3%
on 24 March 1993	2.30×10^8	± 3%
on 8 April 1993	2.28×10^8	± 3%
Anisotropic Factor[a]	1.11	
ϕ_d[b] [cm^{-2} s^{-1}] at 0.75 m		
on 24 March 1993	3618	
on 8 April 1993	3579	
ϕ_s/ϕ_d[c] at 0.75 m	2.8%	
ϕ[d] [cm^{-2} s^{-1}] at 0.75 m		
on 24 March 1993	3720.9	
on 8 April 1993	3680.7	
H_d[e] [mrem h^{-1}] at 0.75 m		
on 1 May 1990[a]	926.1	
on 24 March 1993	433.66	
on 8 April 1993	429.02	
H_s/H_d[f] at 0.75 m	1.05%	
H[g] [mrem h^{-1}] at 0.75 m		
on 1 May 1990[a]	934.6	
on 24 March 1993	438.23	
on 8 April 1993	433.54	

[a] From SLAC-TN-91-3, October 1991.

[b] Direct fluence rate $\phi_d = NF/4\pi r^2$, where N = neutron emission rate, F = anisotropic factor, and r is the detector-to-source distance in cm.

[c] Scattered/direct fluence ratio (ϕ_s/ϕ_d) is estimated from R.B. Schwartz and C.M. Eisenhauer, "Procedures for Calibrating Neutron Personnel Dosimeters," NBS Special Publication 633 (1982). The height for both the detector and source in centimeters was 226.5.

[d] Total fluence rate $\phi = \phi_d + \phi_s$.

[e] Direct dose equivalent rate $H_d = \phi_d h_\phi$, where h_ϕ is the fluence-to-dose equivalent conversion factor. For reference, see note a.

[f] Scattered/direct dose equivalent ratio (H_s/H_d). Same derivation method as note c.

[g] Total dose equivalent rate $H = H_d + H_s$.

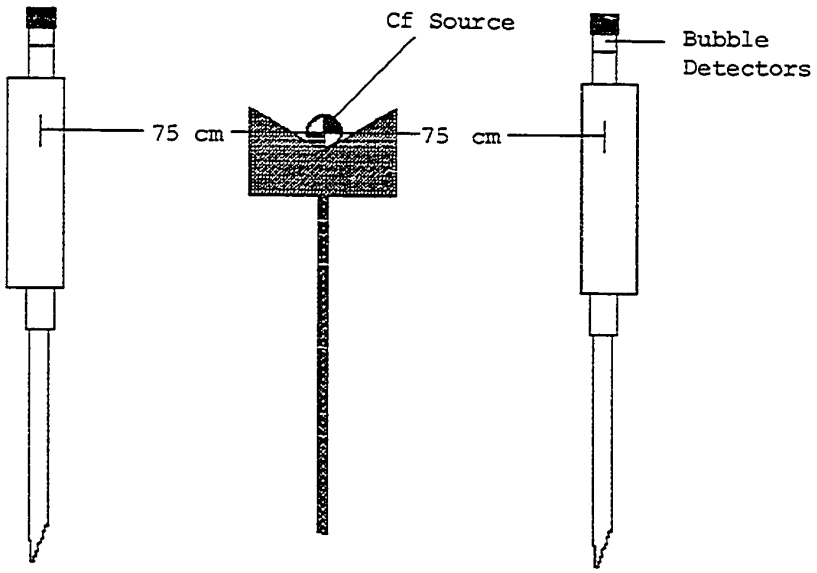

Figure 6.1. Front view of the ^{252}Cf experimental setup.

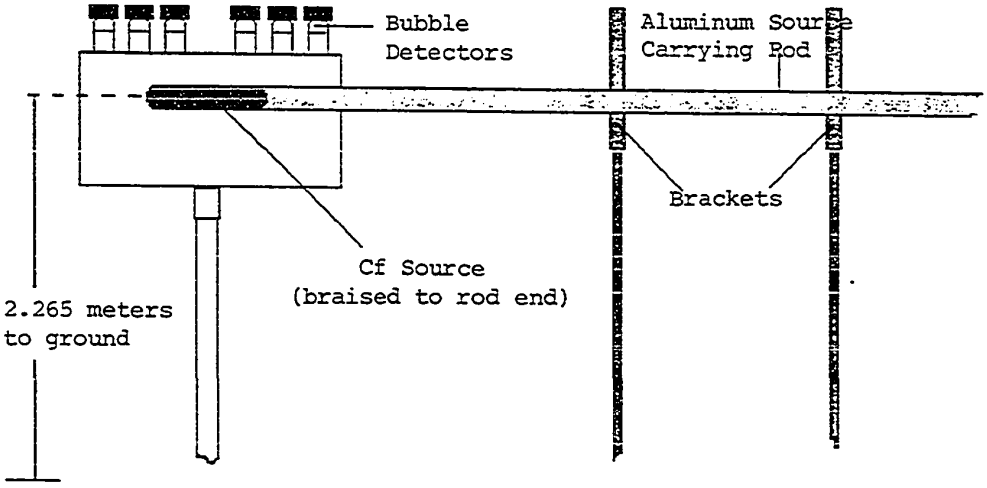

Figure 6.2. Side view of the ^{252}Cf experimental setup.

14 minutes, depending upon which group was being irradiated. Irradiation times were calculated in the same manner as that for the ^{238}PuBe exposures.

BIBLIOGRAPHY

[1] C.M. Eisenhauer, J.B. Hunt, and R.B. Schwartz, "Calibration Techniques for Neutron Personal Dosimetry," Radiat. Prot. Dosim. 10, 44 (1985).

[2] International Organization for Standardization, "Neutron Reference Radiations for Calibrating Neutron Measuring Devices used for Radiation Protection Purposes and for Determining Their Response as a Function of Neutron Energy," ISO Report No. 8529, (1986).

[3] N.E. Hertel and J.C. McDonald, "Calculations of Anisotropy Factors and Dose Equivalents for Unmoderated ^{252}Cf Sources," Radiat. Prot. Dosim., 32, 77 (1990).

[4] J.C. Liu, T.M. Jenkins, R.C. McCall, and N.E. Ipe, "Neutron Dosimetry at SLAC: Neutron Sources and Instrumentation," Stanford Linear Accelerator Center Publication No. SLAC-TN-91-3 (1991).

Chapter VII

RESULTS AND DISCUSSION

7.1 SENSITIVITY CHECK OF THE BDS

Analysis of the ^{238}PuBe BDS data revealed a variability in sensitivity of the BDS over the duration of the study. Aside from the BDS-10 group, which maintained a reasonably constant sensitivity, the sensitivity of the remaining groups (BDS-100s, BDS-600s, BDS-1000s, BDS-2500s, and BDS-10000s) fluctuated to varying degrees, with the greatest fluctuations occurring in the BDS-1000 group. These results are shown in figures 7.1 through 7.7, where the averaged responses (normalized to the check of 5 Feb) were graphed as a function of the date of exposure for the BDS-10s through BDS-10000s respectively. The dotted/dashed lines connecting the data points in figures 7.1 through 7.7 serve merely as visual aids. Combining the data from two irradiation periods results in a smaller degree of sensitivity fluctuations, which is due to more favorable counting statistics. This statistical effect is depicted as the last data point (check number 5) in each figure, and represents the combination of the data from checks 3 (2 Jun) and 4 (3 Jun).

An alternate method of checking the variation in sensitivity is to determine the ratio of the "reference" dose equivalent rate (H_{total}) calculated from the ^{238}PuBe source to the dose equivalent determined from the BDS data. The fluence

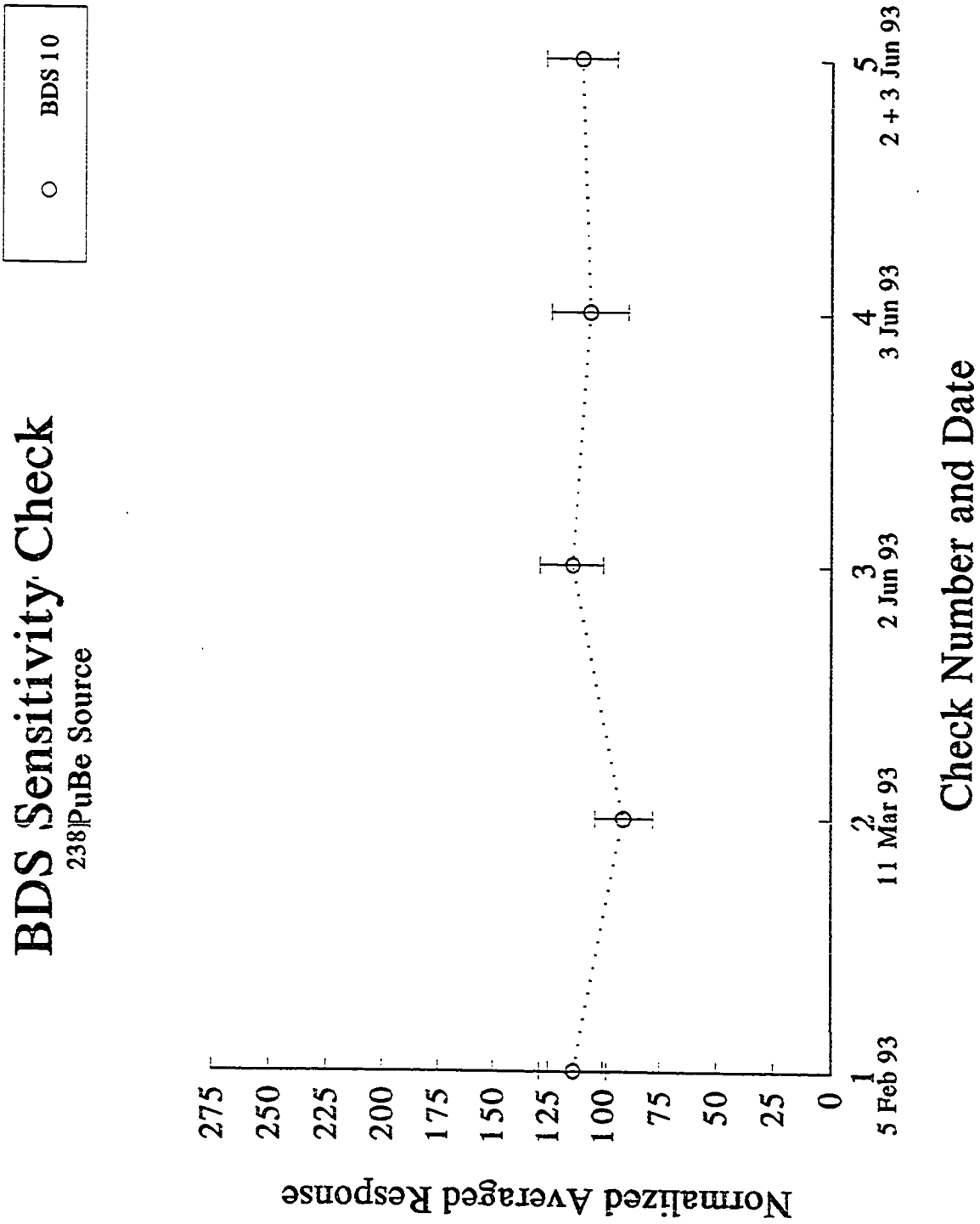

Figure 7.1. Results of the sensitivity variation checks for the BDS-10 at intervals throughout the study.

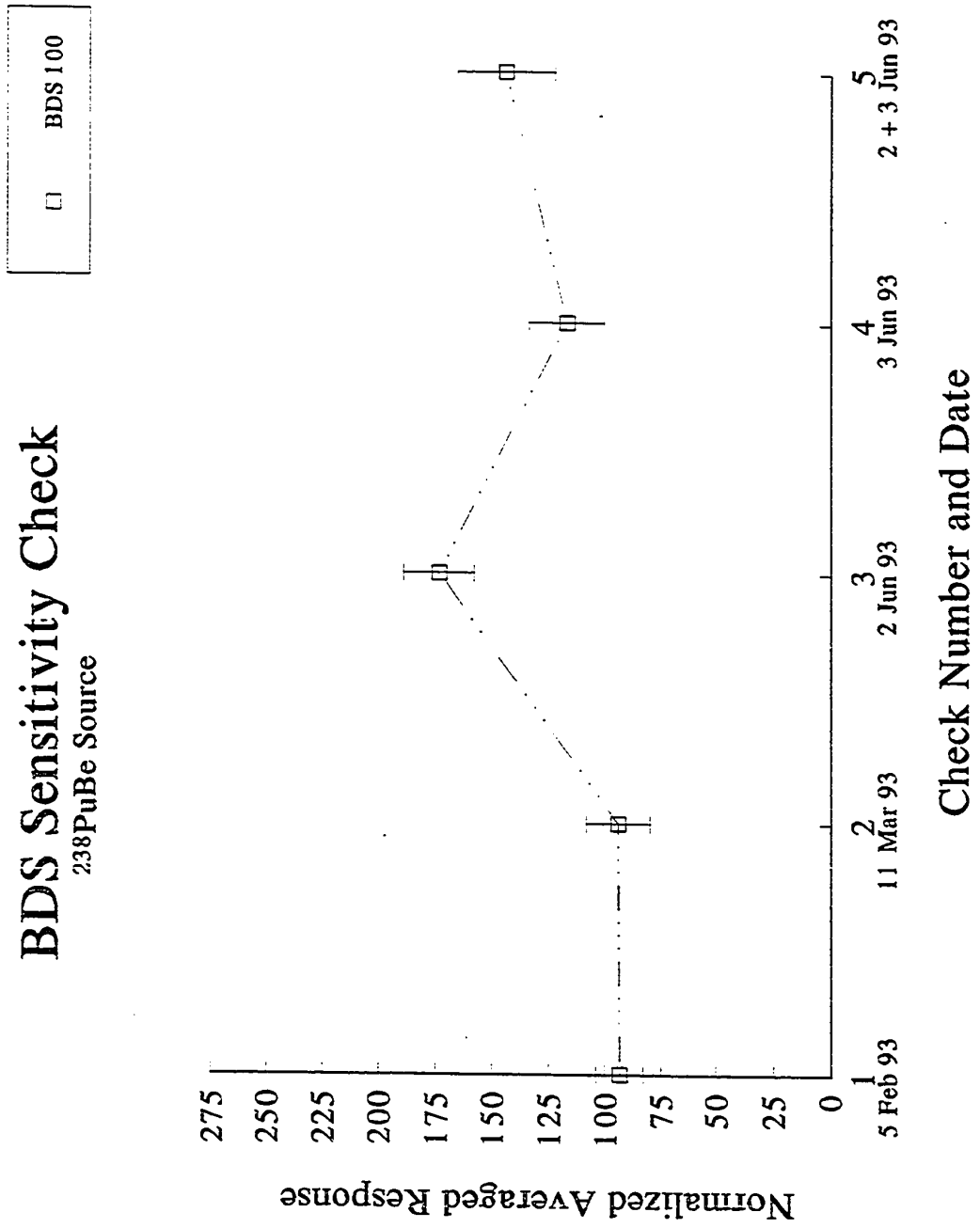

Figure 7.2. Results of the sensitivity variation checks for the BDS-100 at intervals throughout the study.

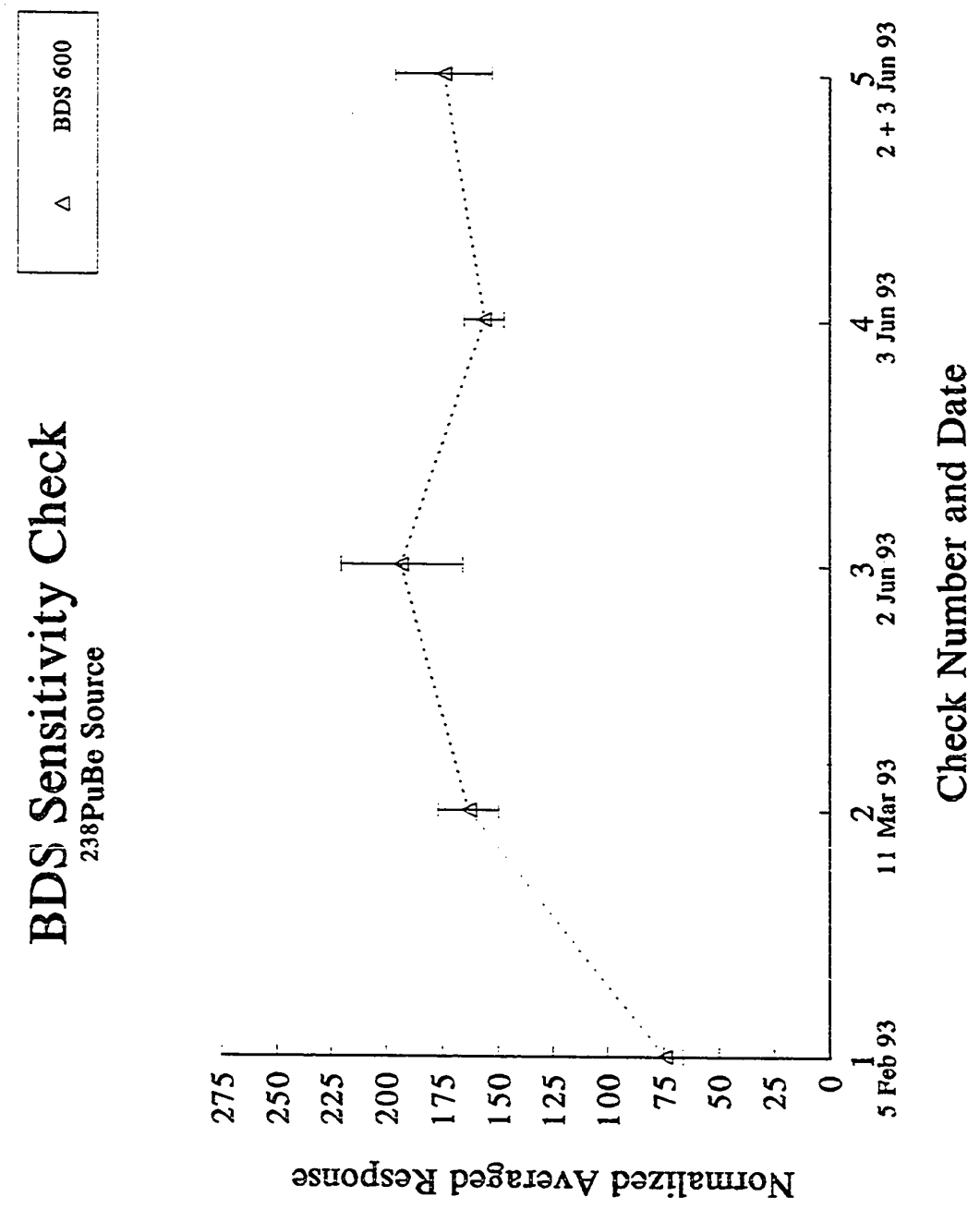

Figure 7.3. Results of the sensitivity variation checks for the BDS-600 at intervals throughout the study.

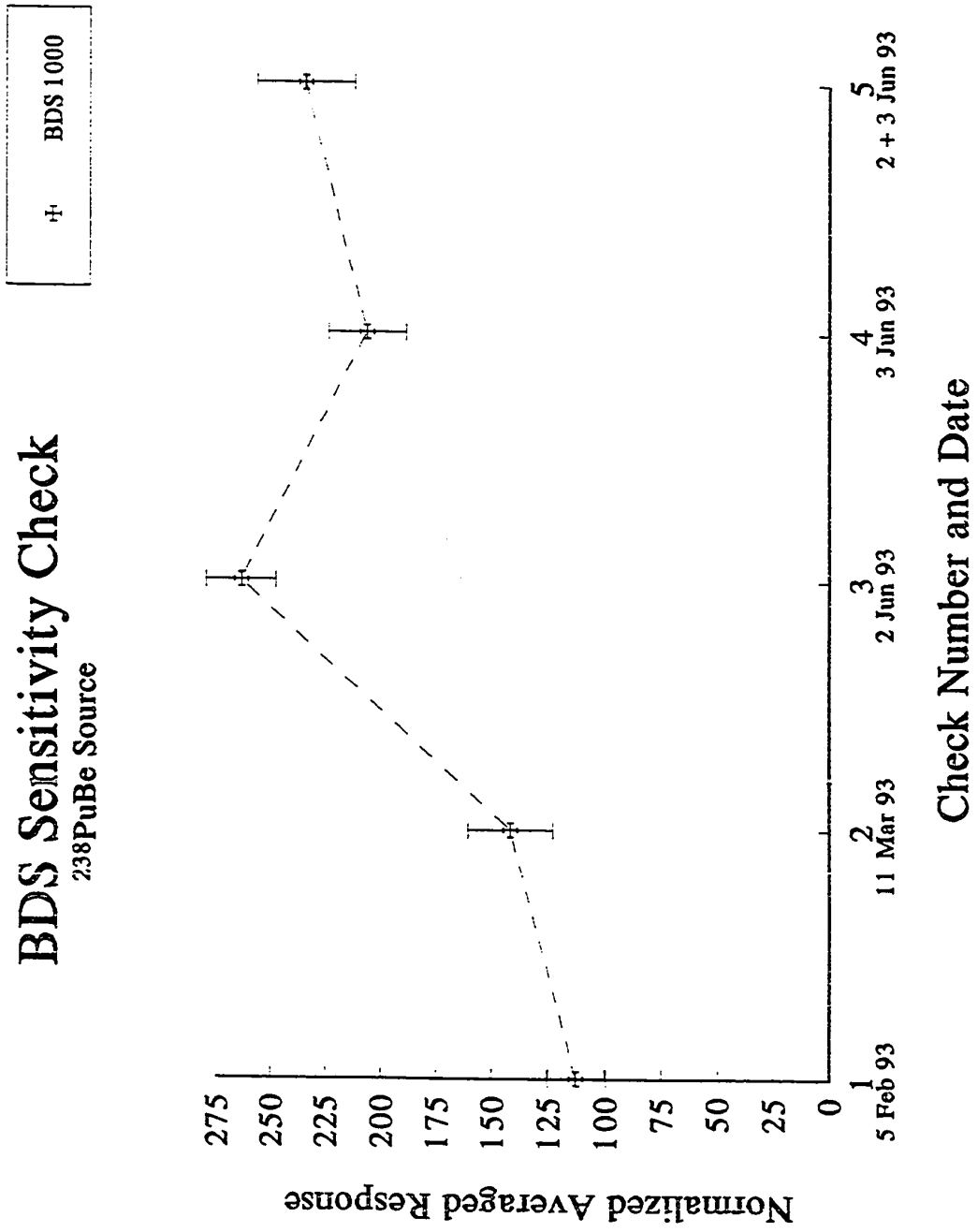

Figure 7.4. Results of the sensitivity variation checks for the BDS-1000 at intervals throughout the study.

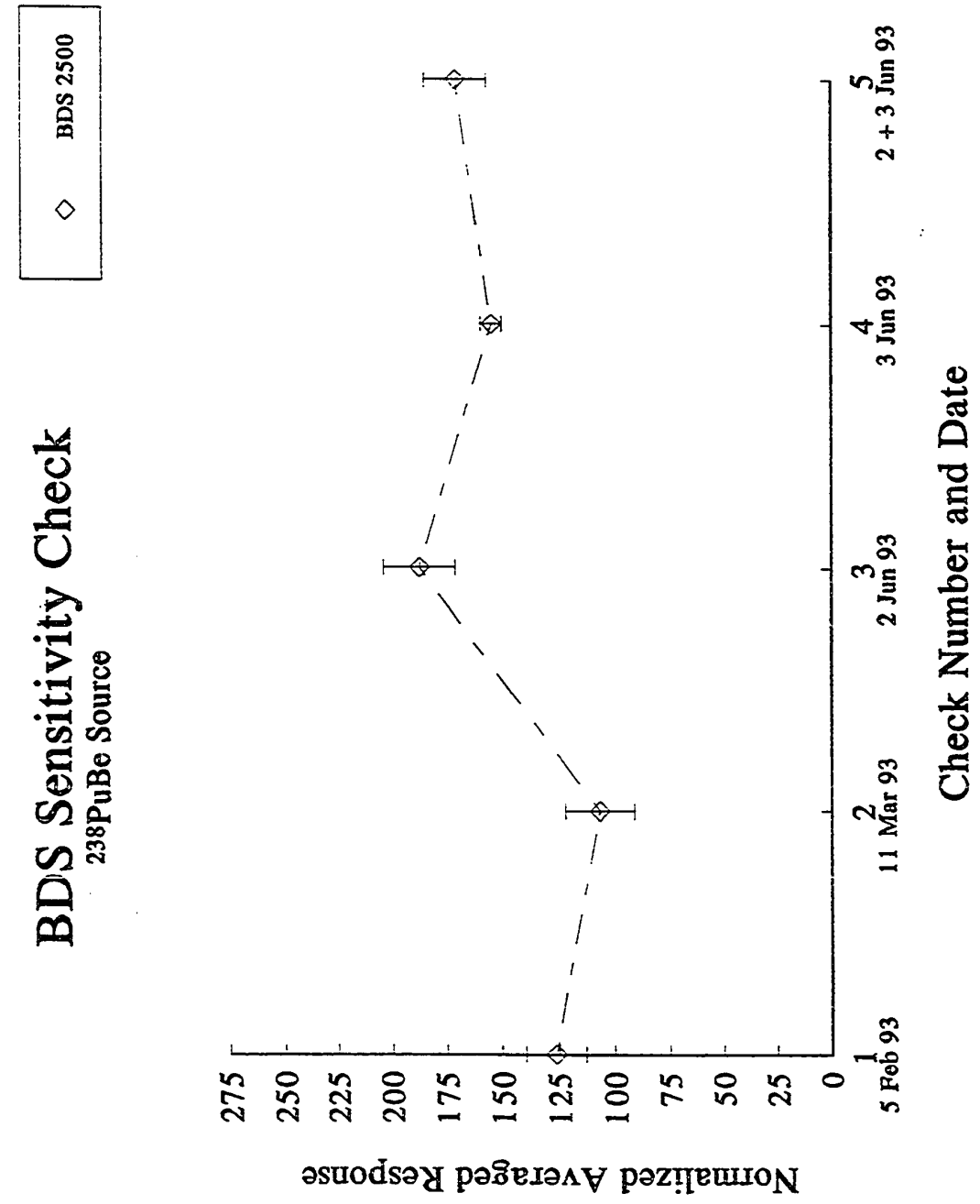

Figure 7.5. Results of the sensitivity variation checks for the BDS-2500 at intervals throughout the study.

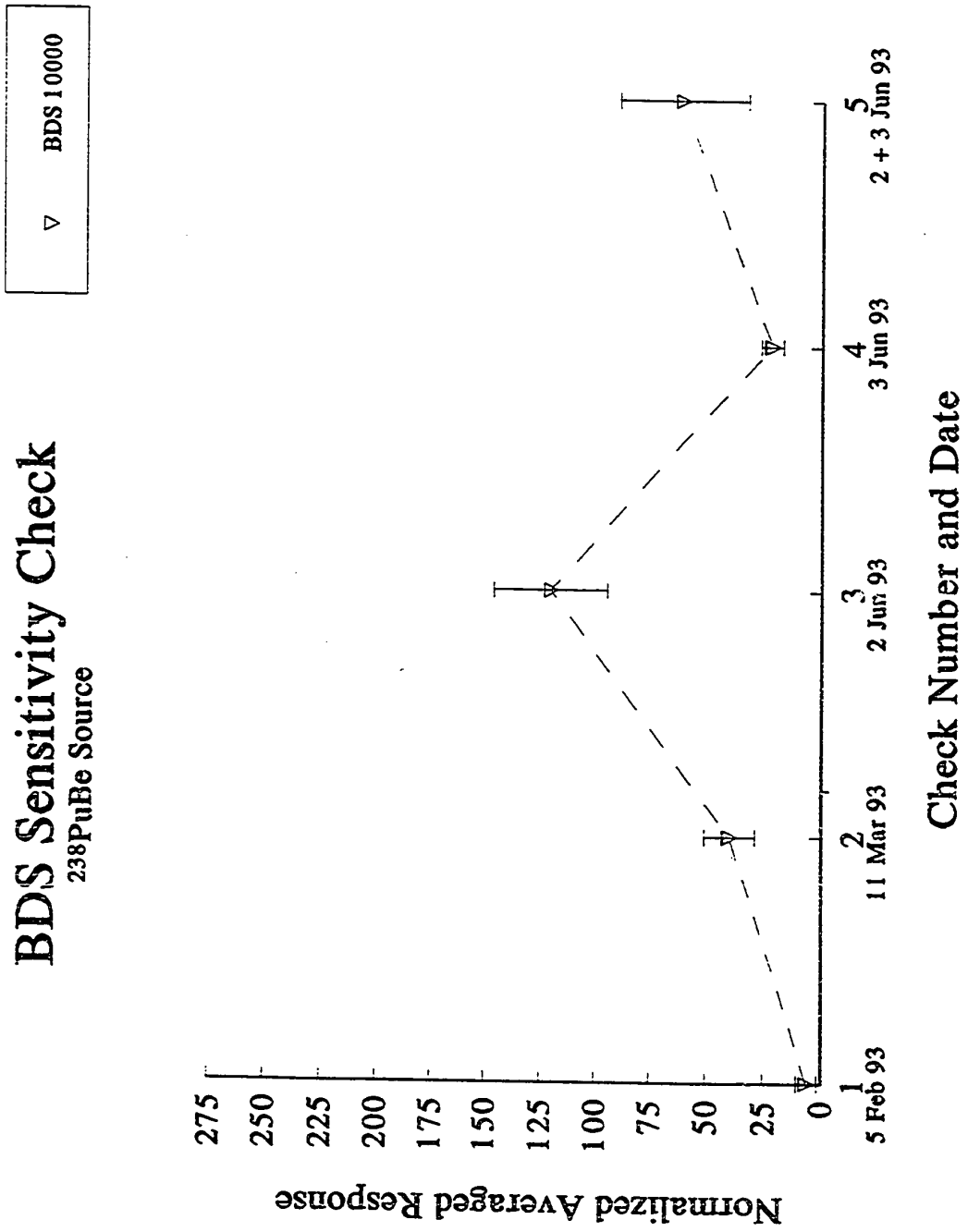

Figure 7.6. Results of the sensitivity variation checks for the BDS-10000 at intervals throughout the study.

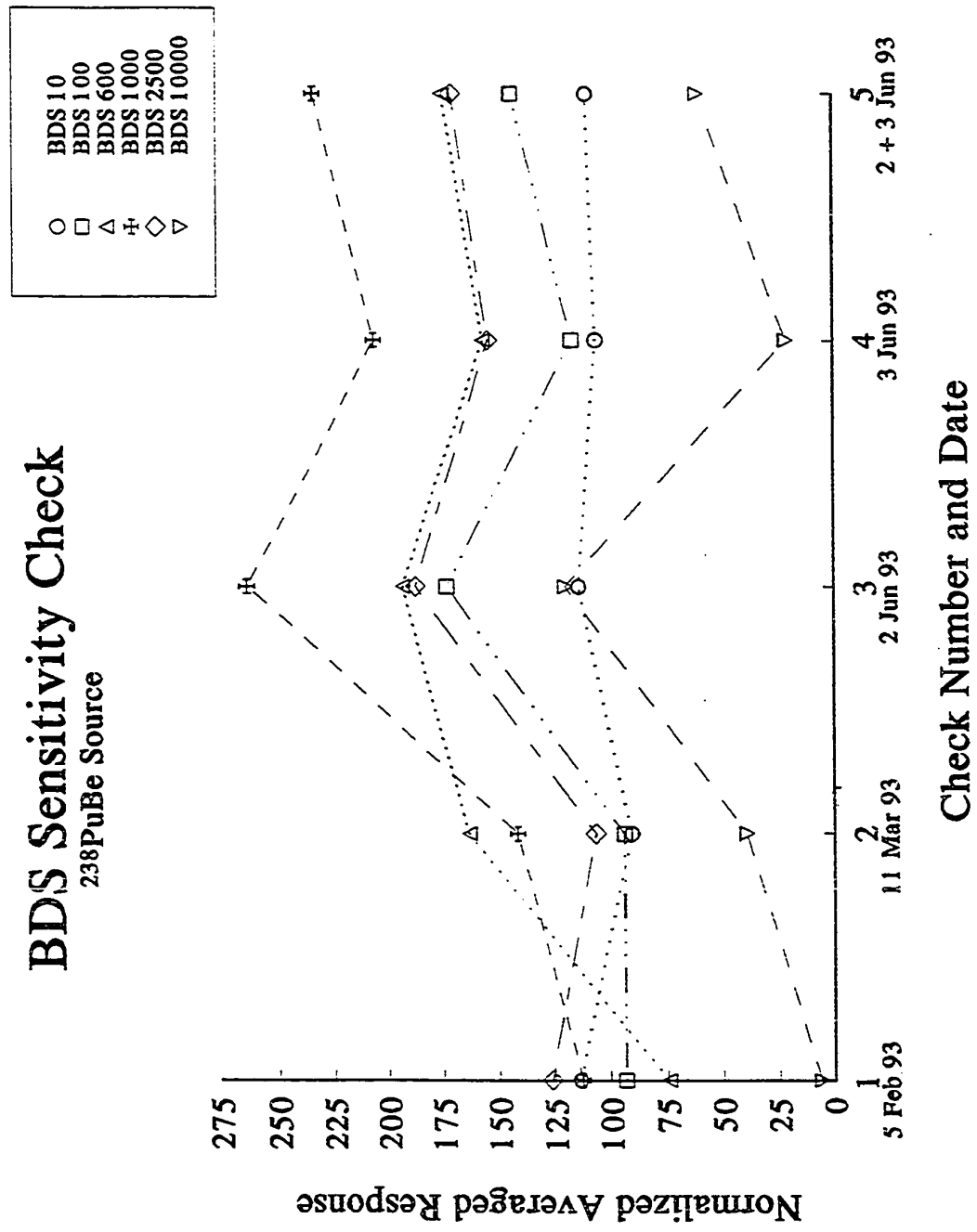

Figure 7.7. Collective results of the sensitivity variation checks for all energy groups of the BDS.

to dose equivalent conversion factors (h_i) for each energy interval of the BDS for both a constant flux assumption and the assumption that the flux varies as 1/E were calculated as described in Appendix C. The fluence for each group (N_i or ϕ_i) as determined from the spectral stripping method (Appendix D) was then multiplied by the appropriate conversion factor and summed, such that the BDS PuBe dose equivalent (H) was found by

$$H = \sum_{i=1}^{6} \phi_i h_i \qquad (7.1)$$

The "reference" dose equivalent rate, $H_{reference}$ (from Table 5.1), was converted to rem/hour, then multiplied by the irradiation time in seconds (this was the time all of the groups had been "normalized" to - the irradiation times of the BDS-10s and BDS-10000s) and divided by 3600 seconds/hour. The ratio of the two dose equivalents was then taken ($H/H_{reference}$) as a measure of how much the sensitivity varied over time. These results are presented in Table 7.1 and also graphed in Figure 7.8.

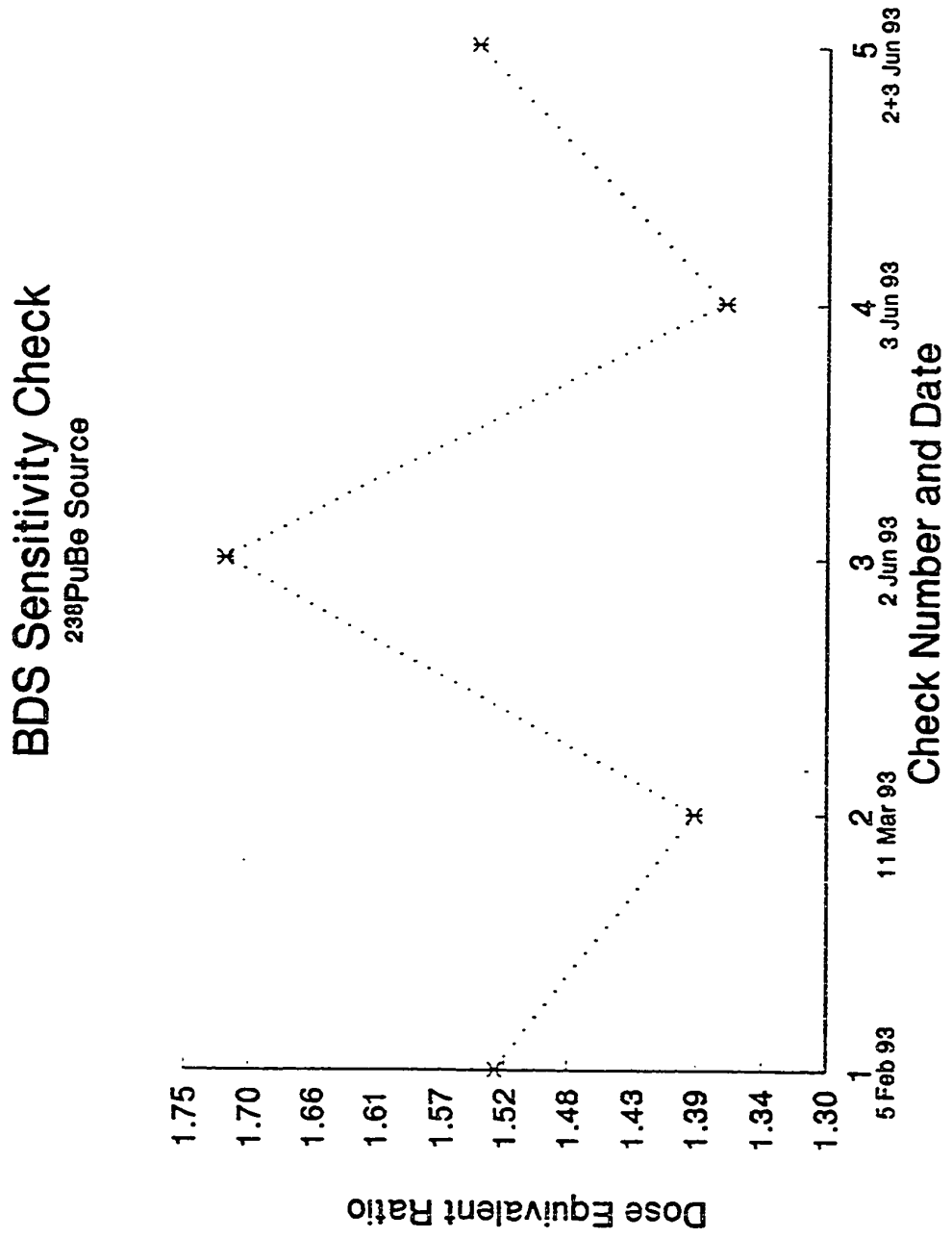

Figure 7.8. BDS sensitivity variations as the ratio of dose equivalents ($H/H_{reference}$) of the BDS with the $^{238}PuBe$ neutron source. The dotted lines connecting the data points serve no purpose other than as a visual aid.

Table 7.1

Sensitivity Check as a Ratio of Dose Equivalent (DE)

Check Date	Reference DE	BDS 1/E DE	Ratio BDS/Reference[a]
5 Feb	0.1053	0.1613	1.532
11 Mar	0.1048	0.1458	1.391
2 Jun	0.1238	0.2132	1.721
3 Jun	0.1238	0.1696	1.370
2+3 Jun	0.1238	0.1911	1.544

[a] These were the values graphed in Figure 7.8.

7.2 PUBE SPECTRA OBTAINED FROM THE BDS

The spectral stripping method was applied to the BDS ^{238}PuBe data and plotted as the logarithm of the fluence versus neutron energy. These results are presented as Figures 7.9(a) through 7.9(e). The absence of the lower energy terms (0.01, 0.1, 0.6, and sometimes 1.0 MeV) in Figures 7.9(a) through 7.9(e) is attributed to the fluence being "forced" to zero due to the non-negativity conditions imposed by the spectral stripping method. For comparison, the neutron spectra of the same ^{238}PuBe source (MRC-426) obtained with multispheres and a source-to-detector distance of 80 cm is shown in Figure 7.10 [1]. The data for this spectra are given in Appendix B.

The difference in spectra between the 5 Feb check and the 11 Mar check could possibly be attributed to the fact that the

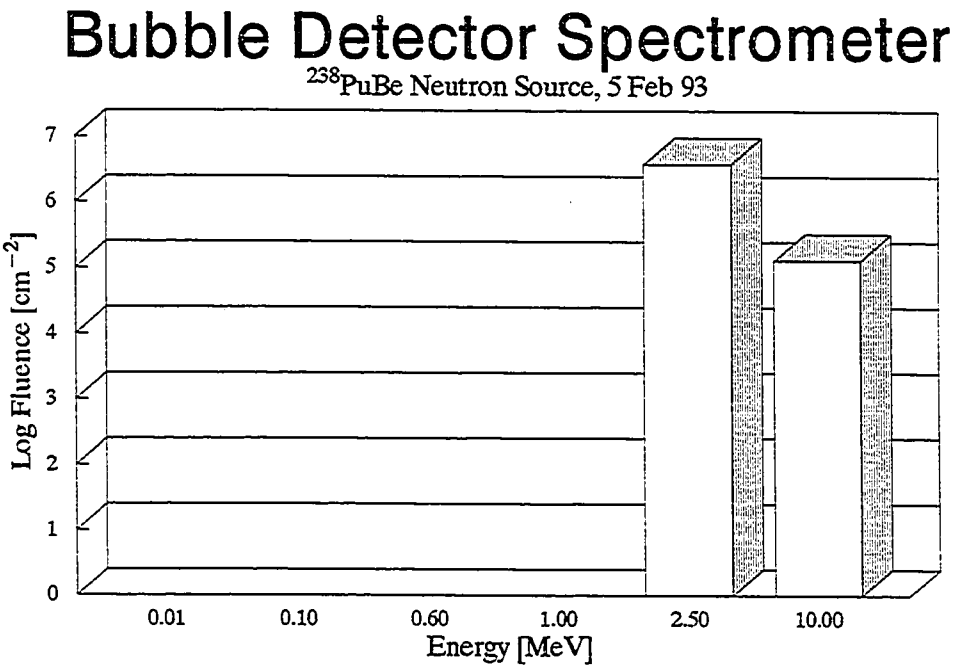

Figure 7.9(a) (above) and Figure 7.9(b) (below). Logarithm of fluence versus neutron energy for the ^{238}PuBe source for the the sensitivity check of 5 Feb (7.9(a)) and 11 Mar (7.9(b)). The fluence was calculated via the spectral stripping method.

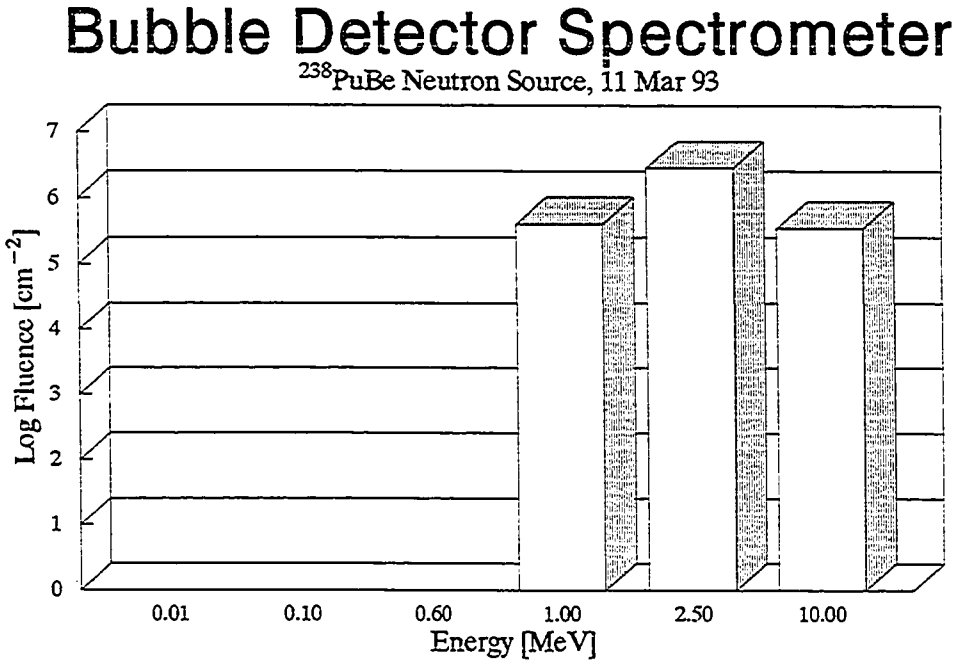

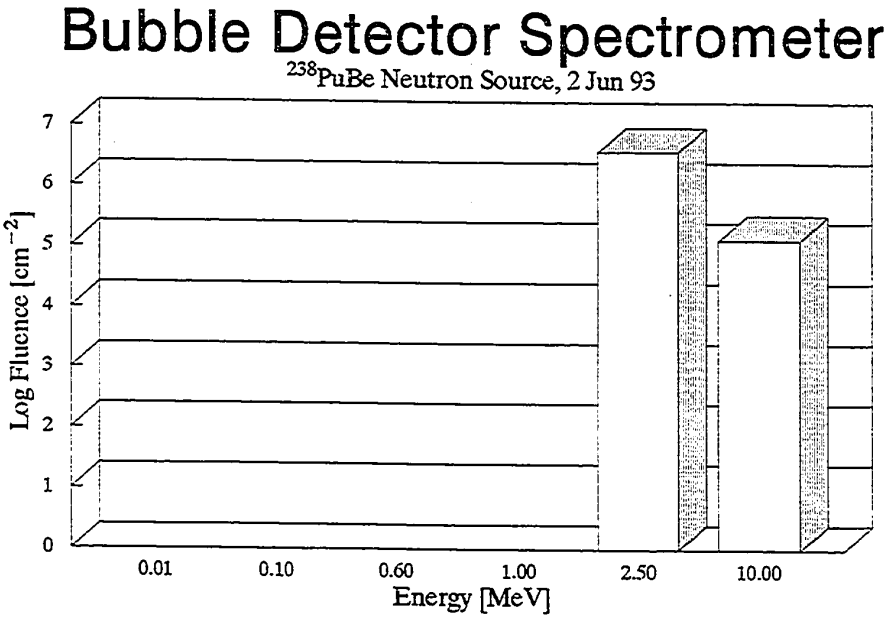

Figure 7.9(c) (above) and Figure 7.9(d) (below). Logarithm of fluence versus neutron energy for the ^{238}PuBe source for the the sensitivity check of 2 Jun (7.9(c)) and 3 Jun (7.9(d)). The fluence was calculated via the spectral stripping method.

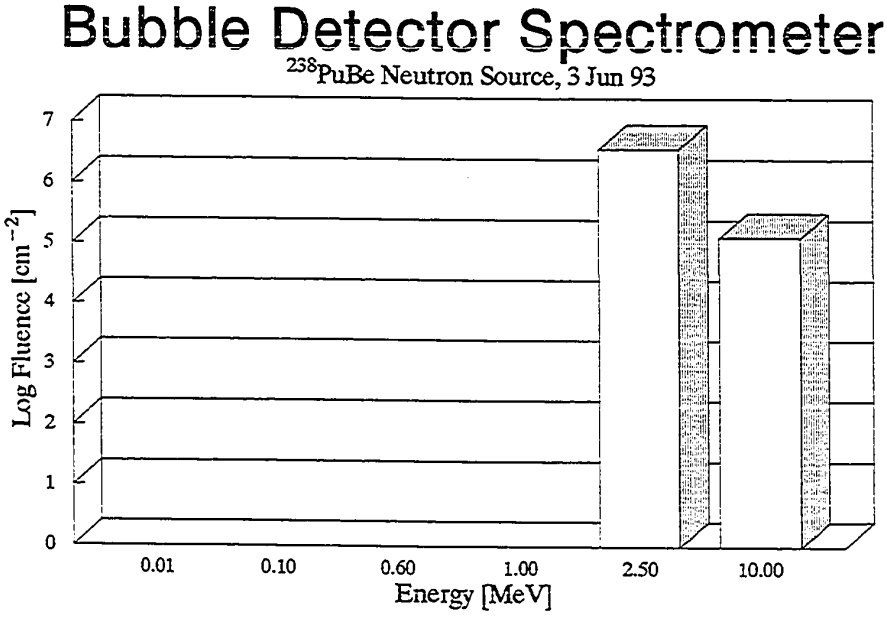

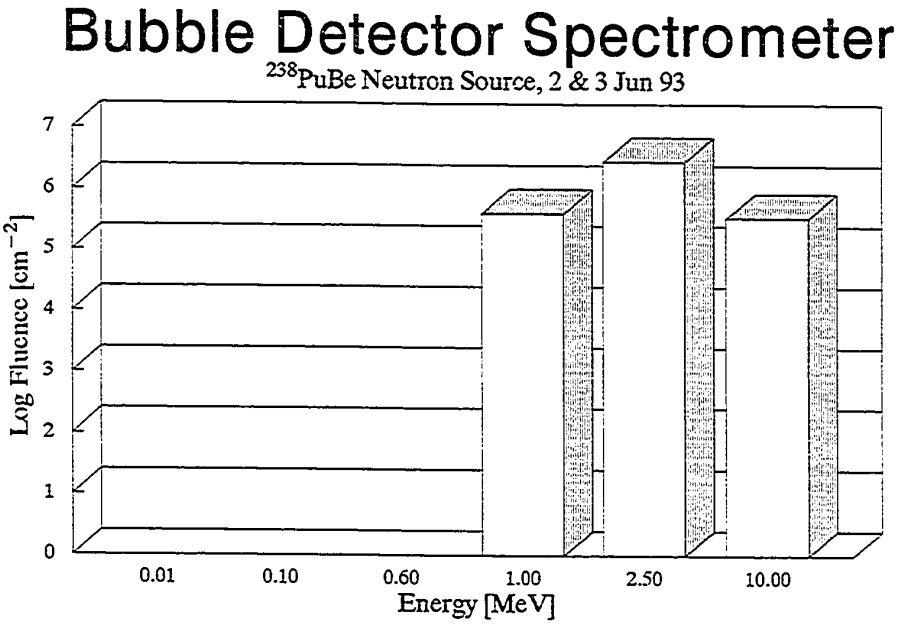

Figure 7.9(e). Logarithm of fluence versus neutron energy for the ^{238}PuBe source for the combination of the data from the sensitivity checks of 2 Jun (7.9(c)) and 3 Jun (7.9(d)). The fluence was calculated via the spectral stripping method.

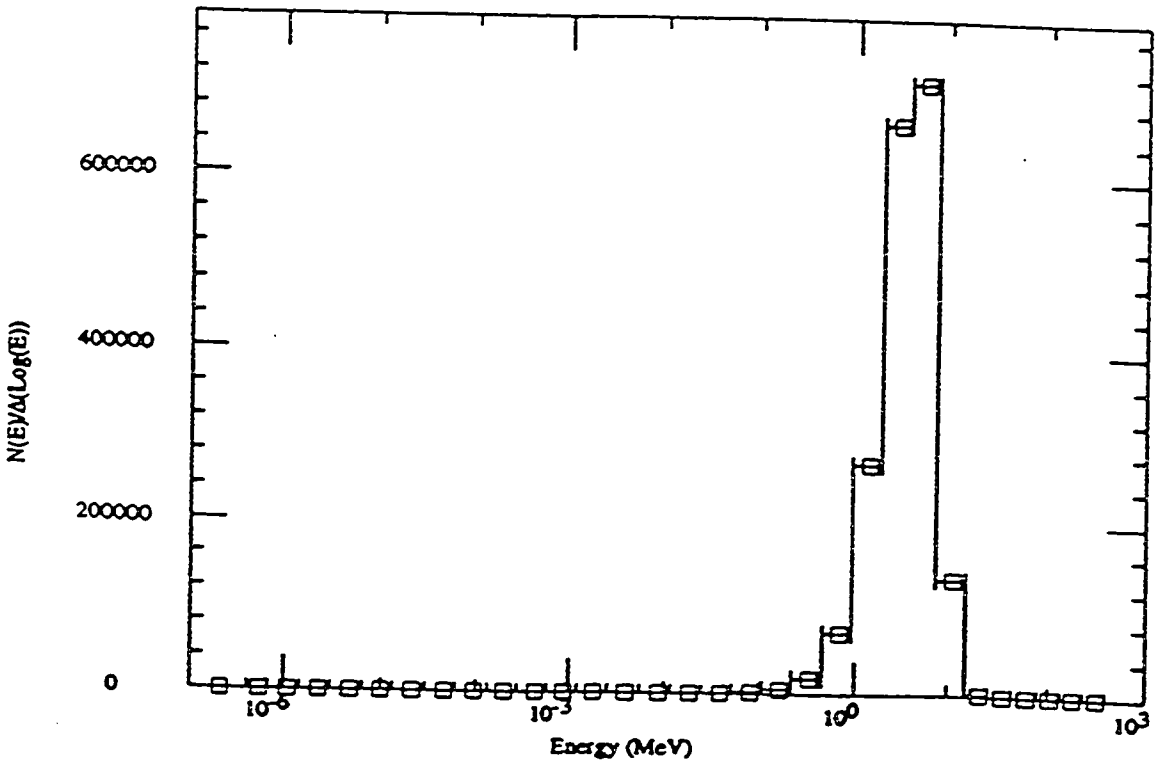

Figure 7.10. The spectrum of the ^{238}PuBe source (MRC-426) obtained with Bonner Multispheres and the BUNKI code. The source-to-detector-distance was 80 cm. The data in columns below represent the output from BUNKI for each of the 31 bins (from Vylet [1]).

BIN NO.	ENERGY MAX (MEV)	FLUENCE MEVT/CM2	FLUENCE N/CM2/LETH	DOSE (RAD)	DOSE EQV. (REM)	DOSE EQV. (% OF TOTAL)
1	4.140E-07	9.530E-05	5.894E-05	5.013E-14	1.097E-13	5.021E-10
2	6.826E-07	5.648E-05	2.601E-04	3.439E-14	6.959E-14	3.185E-10
3	1.645E-06	9.103E-05	2.795E-04	5.621E-14	1.142E-13	5.225E-10
4	3.059E-06	1.940E-04	3.192E-04	6.378E-14	1.293E-13	5.920E-10
5	6.476E-06	1.337E-04	4.103E-04	8.113E-14	1.640E-13	7.507E-10
6	1.371E-05	2.182E-04	6.699E-04	1.311E-13	2.643E-13	1.210E-09
7	2.902E-05	7.236E-04	2.191E-03	4.260E-13	8.527E-13	3.903E-09
8	6.144E-05	2.344E-03	7.195E-03	1.391E-12	2.762E-12	1.265E-08
9	1.301E-04	7.740E-03	2.376E-02	4.561E-12	8.987E-12	4.113E-08
10	2.754E-04	2.565E-02	7.877E-02	1.462E-11	2.881E-11	1.319E-07
11	5.929E-04	8.728E-02	2.621E-01	4.770E-11	9.426E-11	4.314E-07
12	1.234E-03	2.860E-01	8.985E-01	1.502E-10	2.975E-10	1.362E-06
13	2.613E-03	9.574E-01	2.938E-00	4.929E-10	9.765E-10	4.470E-06
14	5.531E-03	3.229E+00	9.916E+00	1.641E-09	3.255E-09	1.490E-05
15	1.171E-02	1.096E+01	3.365E+01	5.523E-09	1.106E-08	5.062E-05
16	2.479E-02	3.755E+01	1.153E+02	2.114E-08	5.685E-08	2.602E-04
17	5.247E-02	1.309E+02	4.019E+02	8.688E-08	3.516E-07	1.609E-03
18	1.111E-01	4.701E+02	1.443E+03	3.689E-07	2.245E-06	1.028E-02
19	2.237E-01	1.620E+03	5.331E+03	1.682E-06	1.345E-05	6.155E-02
20	4.508E-01	5.627E+03	1.849E+04	8.181E-06	7.967E-05	3.647E-01
21	9.072E-01	2.152E+04	7.084E+04	4.828E-05	5.165E-04	2.355E+00
22	1.872E+00	8.429E+04	2.679E+05	2.871E-04	2.955E-03	1.353E+01
23	3.679E+00	1.946E+05	6.631E+05	8.210E-04	7.773E-03	3.558E+01
24	7.408E+00	2.161E+05	7.110E+05	1.249E-03	8.800E-03	4.028E+01
25	1.492E+01	4.120E+04	1.355E+05	2.728E-04	1.694E-03	7.753E+00
26	2.581E+01	3.413E+02	1.434E+03	3.105E-06	1.487E-05	6.805E-02
27	4.465E+01	3.743E+00	1.573E+01	3.597E-08	1.658E-07	7.591E-04
28	7.725E+01	4.013E-02	1.686E-01	4.065E-10	1.891E-09	8.656E-06
29	1.336E+02	4.182E-04	1.758E-03	4.755E-12	2.102E-11	9.621E-08
30	2.312E+02	4.277E-06	1.795E-05	6.372E-14	2.367E-13	1.084E-09
31	4.000E+02	4.021E-08	1.689E-07	7.214E-16	2.557E-15	1.170E-11

Table 7.1

Sensitivity Check as a Ratio of Dose Equivalent (DE)

Check Date	Reference DE	BDS 1/E DE	Ratio BDS/Reference[a]
5 Feb	0.1053	0.1613	1.532
11 Mar	0.1048	0.1458	1.391
2 Jun	0.1238	0.2132	1.721
3 Jun	0.1238	0.1696	1.370
2+3 Jun	0.1238	0.1911	1.544

[a] These were the values graphed in Figure 7.8.

7.2 PUBE SPECTRA OBTAINED FROM THE BDS

The spectral stripping method was applied to the BDS ^{238}PuBe data and plotted as the logarithm of the fluence versus neutron energy. These results are presented as Figures 7.9(a) through 7.9(e). The absence of the lower energy terms (0.01, 0.1, 0.6, and sometimes 1.0 MeV) in Figures 7.9(a) through 7.9(e) is attributed to the fluence being "forced" to zero due to the non-negativity conditions imposed by the spectral stripping method. For comparison, the neutron spectra of the same ^{238}PuBe source (MRC-426) obtained with multispheres and a source-to-detector distance of 80 cm is shown in Figure 7.10 [1]. The data for this spectra are given in Appendix B.

The difference in spectra between the 5 Feb check and the 11 Mar check could possibly be attributed to the fact that the

holder for the source differed on those two dates. However, the same holder was used on 11 Mar, 2 Jun and 3 Jun, and great care was taken to exactly reproduce the identical geometry in all checks. The latter two checks (2 Jun and 3 June) shared constant geometry, as the experimental setup was left in place overnight then rechecked the following morning, with the experimental procedure being identical in all other respects. The difference between the spectra of 2 Jun and 3 Jun (and probably the remainder as well) is best explained by the combination of statistics and variability in the detectors' sensitivity (i.e. temperature), particularly the BDS-1000 detectors. The effect of statistics is illustrated in figure 7.9(e), which is the spectra obtained from combining the data from the 2 and 3 Jun checks.

The average neutron energy was calculated for both for a 1/E and a constant E assumption for each energy interval as described in Appendix E. The results are presented in Table 7.2.

Table 7.2

Average Energy of the ^{238}PuBe Neutron Source

Experiment Date	$E_{Average}$ 1/E [MeV]	$E_{Average}$ Const. Flux [MeV]	Reference Value[a] [MeV]
5 Feb	5.7	6.5	4.2
11 Mar	5.89	6.9	4.2
2 + 3 Jun	5.7	6.4	4.2

[a] From SLAC-TN-91-3

The ^{238}PuBe data was primarily used for sensitivity checking purposes, thus it was not analyzed with BUNKI.

7.3 ANALYSIS OF ^{252}CF BDS DATA - SPECTRAL STRIPPING METHOD

The responses of each of the energy groups of the BDS were normalized with respect to the longest irradiation time (that of the BDS-10s and BDS-10000s). The fluence was calculated via the spectral stripping method and plotted as the logarithm of the fluence versus neutron energy. Results are presented in figure 7.11.

Based solely on counting statistics, the "starting" error for unfolding this spectrum by the stripping method was approximately 45%, as there were only 5 bubbles in the entire BDS-10000 group of six detectors. This is attributed to the fact that there are very few neutrons at 10 MeV and none above

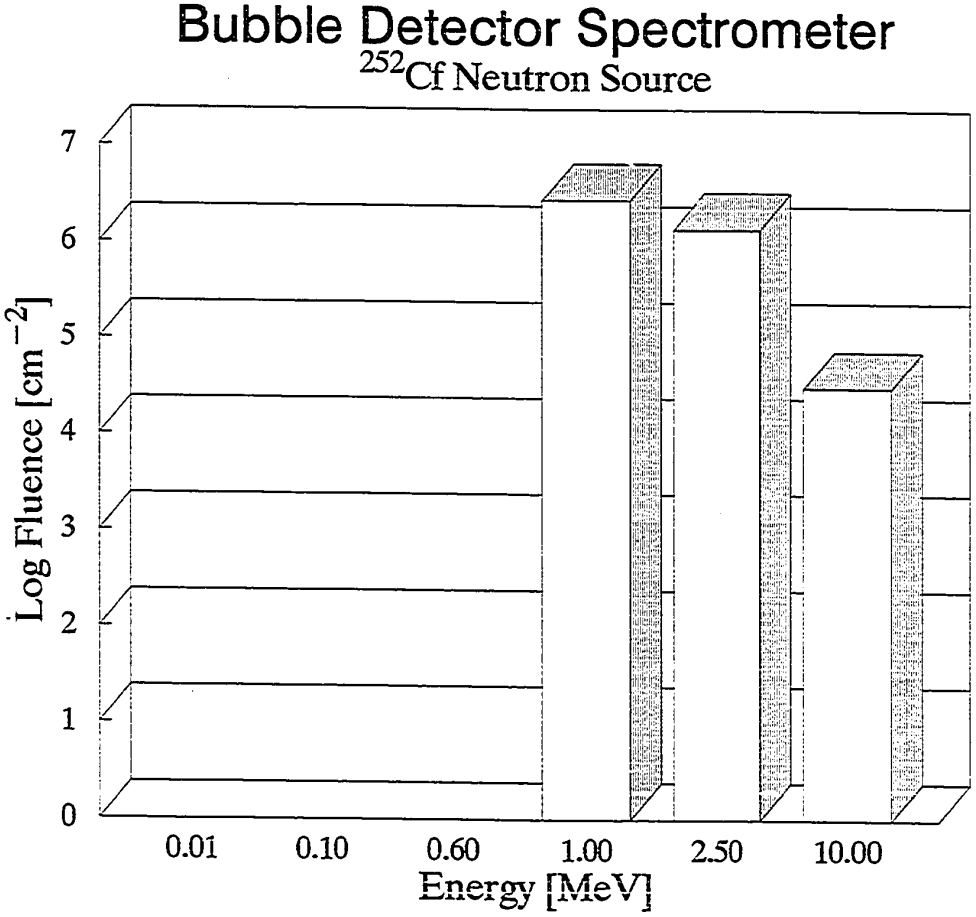

Figure 7.11. Logarithm of the fluence versus neutron energy for the ^{252}Cf source. The fluence was calculated via the spectral stripping method.

10 MeV to be measured when using a fission source, such as ^{252}Cf.

The responses of the individual BDS threshold groups from the ^{252}Cf exposures are presented in Table 7.3. The error terms presented in the "average number of bubbles per second" column represent the statistical uncertainty of the total number of bubbles counted for all six detectors in each respective group. The last column gives the number of bubbles per second for detectors of unit sensitivity. This term was calculated by dividing the average number of bubbles by the average detector sensitivity.

The average neutron energy was calculated for a 1/E and a constant E assumption for each energy interval (Appendix D). The average energy results were 2.99 MeV (1/E) and 3.348 MeV (constant E), representing a 44% and 62% change from the reference value of 2.07 MeV given for an unmoderated Savannah River encapsulated ^{252}Cf source from Monte Carlo calculations by Hertel and McDonald [2].

Table 7.3

Responses of BDS Groups from ^{252}Cf Measurement at 75 cm

Detector Group I.D.	Average # Bubbles s^{-1}	Average Detector Sensitivity[a]	Average Standardized Response s^{-1}
BDS-10	0.091 ± 5%	0.565 ± 10%	0.161 ± 15%
BDS-100	0.185 ± 5%	1.16 ± 10%	0.158 ± 15%
BDS-600	0.433 ± 4%	2.33 ± 10%	0.186 ± 14%
BDS-1000	0.416 ± 6%	3.98 ± 10%	0.104 ± 16%
BDS-2500	0.301 ± 7%	5.68 ± 10%	0.053 ± 17%
BDS-10000	0.006 ± 45%	0.59 ± 10%	0.010 ± 55%

[a] Provided by the manufacturer (BTI).

7.4 ANALYSIS OF ^{252}CF MULTISPHERE DATA - THE BUNKI CODE

As mentioned in Chapter III, numerous trials were run with various response matrices, smoothing factors, starting temperatures, and varying numbers of iterations, in an effort to determine which conditions produced the "best fit" of the Cf multisphere/TLD data. To determine the "best" number to use for iterative purposes, the BUNKI program was run with 0, 50, 100, 200, 500, 750, and 1000 iterations for the multisphere ^{252}Cf data. The results are presented in Table 7.4. Closest agreement to the average energy value of 2.07 MeV was obtained with 750 iterations for the multisphere/TLD BUNKI data in Table 7.4.

Table 7.4

Effect on the Multisphere Neutron Spectra with Increasing Iterations in the BUNKI Program

Number of Iterat.	Neutron Fluence[a] [cm^{-2}]	Average Energy [MeV]	Dose Equivalent [rem]	Fitting Error[b] [%]
0	1.167	2.145	3.762×10^{-8}	7.063
50	1.147	1.929	3.665×10^{-8}	4.868
100	1.149	1.877	3.666×10^{-8}	4.498
200	1.152	1.869	3.673×10^{-8}	4.303
500	1.165	1.985	3.695×10^{-8}	4.053
750	1.175	2.103	3.718×10^{-8}	3.898
800	1.177	2.127	3.723×10^{-8}	3.870
1000	1.184	2.224	3.743×10^{-8}	3.768

[a] Calibration factor of unity (no calibration).

[b] This error indicates the agreement of BUNKI's solution with the experimental data, not the reliability of the solution.

To determine the calibration factor to be input into BUNKI for the multisphere/TLD data, the value of the direct fluence rate (Table 6.1) was multiplied by the irradiation time as follows:

$$(3579\ cm^{-2}s^{-1})\ (3600\ s\ hr^{-1})\ 1\ hr = 1.288 \times 10^{7}\ cm^{-2}. \quad (7.2)$$

The direct fluence rate was used, as separate scattering

corrections had already been applied to the input data from the multispheres using the method of Sun [3]. The value obtained in equation 7.2 was divided by the total fluence obtained from BUNKI output for the multispheres with a calibration factor of unity (not calibrated) for the case of 750 iterations, hence

$$(1.288 \text{ X } 10^7)/1.175 = 1.096 \text{ X } 10^7. \qquad (7.3)$$

This value was input into the BUNKI code as the calibration factor and the program was run with the parameters indicated in the "sample" input file in Appendix A (Table A.2). The resulting unfolded spectrum is presented in Figure 7.12. The "reference" spectrum from a Monte Carlo calculation of a Savannah River encapsulated, unmoderated ^{252}Cf source is presented in figure 7.13 [1].

7.5 ANALYSIS OF ^{252}CF BDS - THE BUNKI CODE

The BDS ^{252}Cf data appeared to diverge further from the reference values as the number of iterations was increased in the BUNKI unfolding. This may be attributed to the response matrix "giant_bubble" utilized in the unfolding code. No corrections for scattering were applied to the BDS BUNKI input data, nor was a calibration factor input, as the responses of the BDSs were already normalized to unit sensitivity. The results for 100 iterations and 750 iterations are shown in

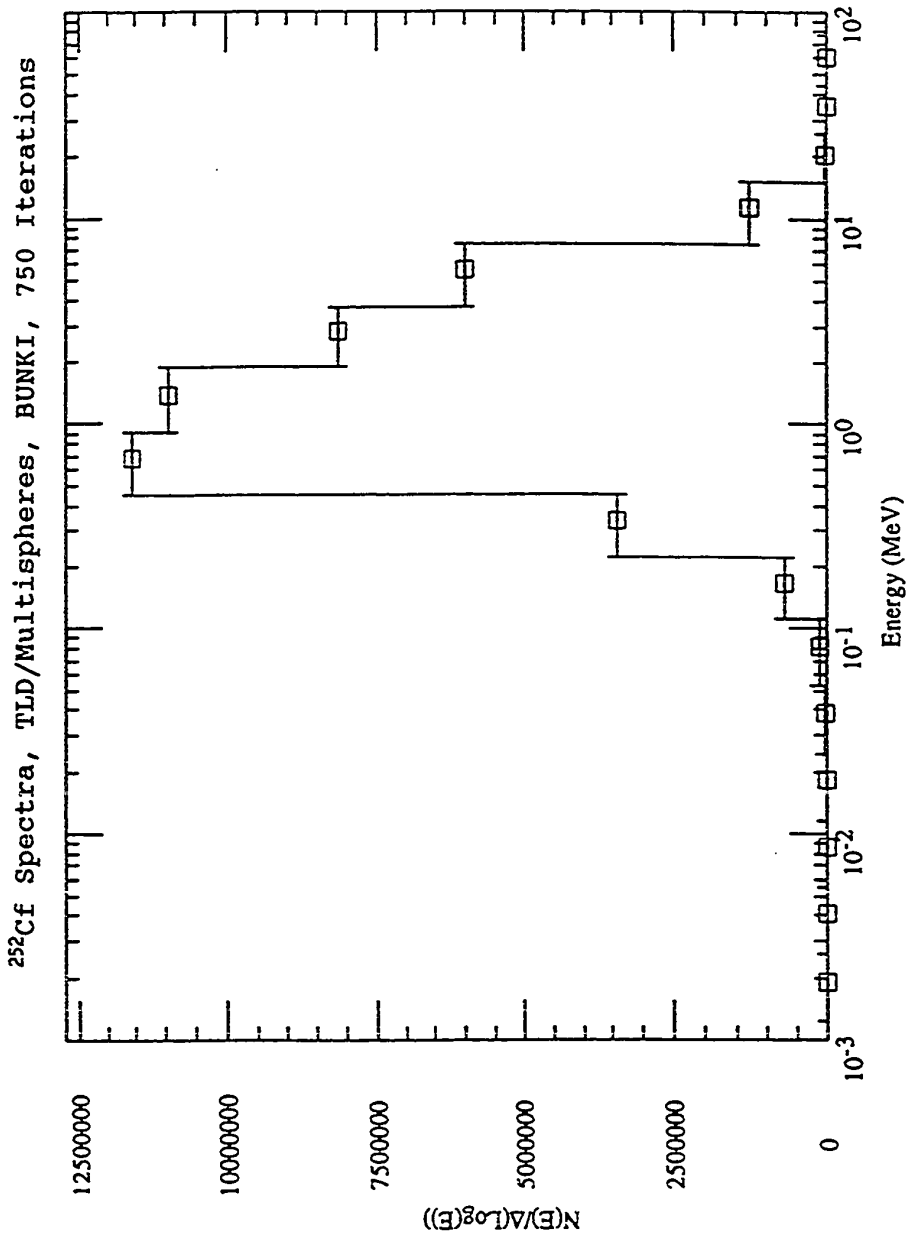

Figure 7.12. The ^{252}Cf neutron spectra obtained from the BUNKI unfolding code for the Bonner multisphere/TLD detectors.

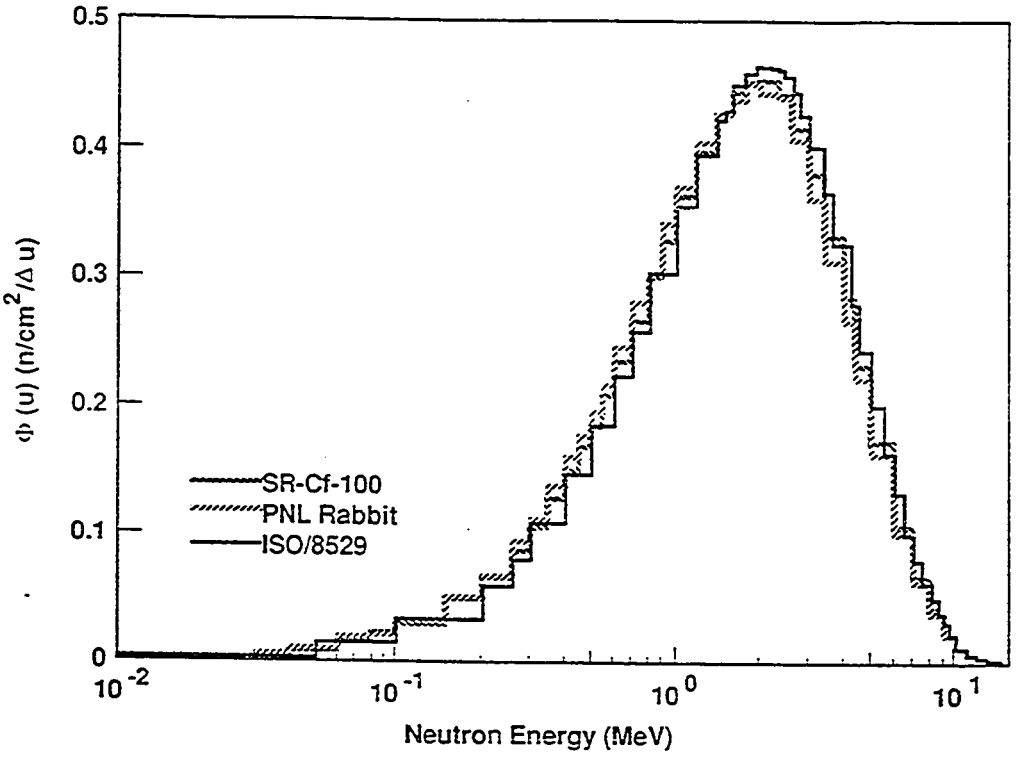

Figure 7.13. Unmoderated ^{252}Cf source fluence spectra, normalized to unit fluence for comparison. The spectrum for the source alone is shown along with the spectrum for the source within its transport capsule (PNL Rabbit) and spectrum from ISO Standard 8529, for reference. From Hertel and McDonald [2].

Table 7.5, and the spectra are presented as Figure 7.14 and 7.15 respectively.

Table 7.5

BUNKI Output of the BDS Neutron Spectra

Number of Iterat.	Neutron Fluence [cm^{-2}]	Average Energy [MeV]	Dose Equivalent [rem]	Fitting Error[a] [%]
100	3.95×10^{6}	2.357	1.437×10^{-1}	3.374
750	4.01×10^{6}	2.287	1.481×10^{-1}	1.904

[a] This error indicates the agreement of BUNKI's solution with the experimental data, not the reliability of the solution.

7.5 ANALYSIS OF MODERATED FOILS METHOD FOR ^{252}Cf

The ^{252}Cf induced activity in the indium foil was counted in the physics laboratory at Varian Associates using a 1 inch diameter Geiger tube with an end window thickness of 1.4 mg/cm^2, connected to a Ludlum Model 2200 Portable Scaler Rate Meter. The Geiger tube assembly was housed within lead shielding to reduce background interference, and coincidence loss rates were negligible at 10,000 cpm. The saturation count rate (C_s) from the flux integrator and rem meter foils was determined in accordance with the procedure given in Appendix II of AAPM Report Number 19 as follows [4]:

$$C_s = \frac{C(\lambda t_c)\exp(\lambda t_w)}{(1-\exp(-\lambda t_i))(1-\exp(-\lambda t_c)} \quad [\text{cps}]$$

where C is the measured count rate corrected for background and counting shelf location, λ is the indium decay constant, t_w is the waiting time from the end of irradiation to the beginning of the counting, t_c is the counting time, and t_i is the irradiation time.

A ^{252}Cf calibration factor for both the flux integrator and remmeter was determined from the method outlined by LaRiviere [5] and multiplied by the respective saturation counts to determine the flux and dose equivalent. The average neutron energy was determined from SLAC-TN-91-3 [6]. The moderated foil method results are summarized with the results from the other methods in Chapter VIII (Summary and Conclusion).

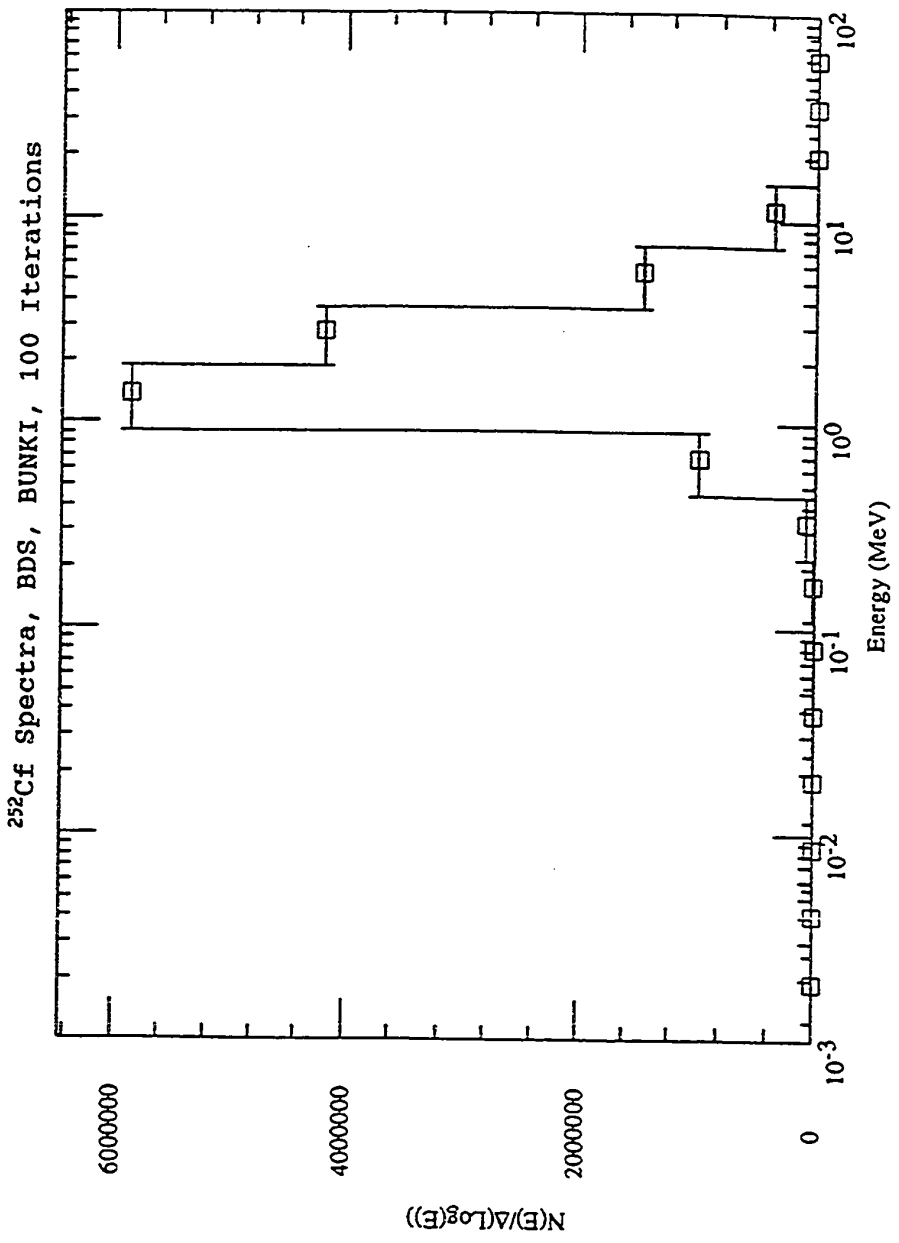

Figure 7.14. The ^{252}Cf neutron spectra obtained from the BUNKI unfolding code for the BDS detectors with 100 iterations.

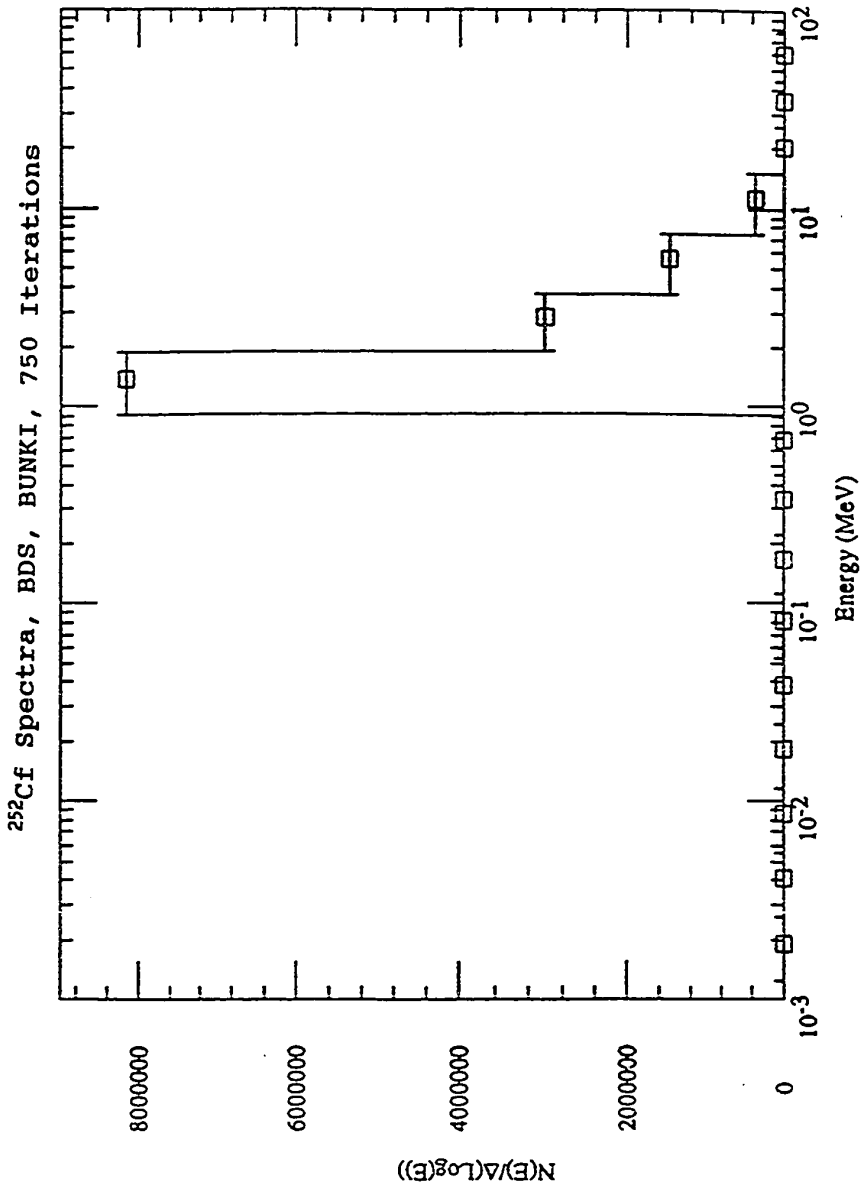

Figure 7.15. The ^{252}Cf neutron spectra obtained from the BUNKI unfolding code for the BDS detectors with 750 iterations.

BIBLIOGRAPHY

[1] V. Vylet, SLAC, 1993 (private communication).

[2] N.E. Hertel and J.C. McDonald, "Calculations of Anisotropy Factors and Dose Equivalents for Unmoderated ^{252}Cf Sources," Radiat. Prot. Dosim., 32, 81 (1990).

[3] R-K. S. Sun, "Investigation of Neutron Scattering for a Multisphere Spectrometer," Health Phys. 59, 327 (1990).

[4] American Association of Physicists in Medicine "Neutron Measurements around High Energy X-Ray Radiotherapy Machines," Report No. 19 (1986).

[5] P.D. LaRiviere, "Neutron energies in medical accelerator rooms," Med. Phys., 12, 769 (1985).

[6] J.C. Liu, T.M. Jenkins, R.C. McCall, and N.E. Ipe, "Neutron Dosimetry at SLAC: Neutron Sources and Instrumentation," Stanford Linear Accelerator Center Publication No. SLAC-TN-91-3 (1991).

Chapter VIII

SUMMARY AND CONCLUSIONS

8.1 SUMMARY OF RESULTS

A comparison of the results of the various methods utilized in this research is presented in Table 8.1. The reference values were taken from Chapter VI, Table 6.1. The total fluence values for each method are normalized to unit time. The total fluence value given for the multisphere [BUNKI] method was obtained by adding a 2.8% scattering factor to the direct fluence value. The direct fluence values given for the BDS (1/E, constant flux, and BUNKI columns) and the flux integrator/remmeter were obtained by subtracting 2.8% from the respective methods' values for the total fluence, where 2.8% represents the scattered/direct fluence ratio, taken from Table 6.1. The percent error listed for the BUNKI methods indicates the consistency of the unfolded solution with the experimental data, and not the reliability of the solution. The percent error given for the flux integrator/remmeter represents the standard deviation of the ratio of flux integrator/remmeter counts.

TABLE 8.1

Results of the Various Methods for the ^{252}Cf Source

		Type of Detector: BDS	BDS	BDS	MULTI– SPHERE/TLD	FLUX INTGR. REM METER
Quantity Determined	Reference Values	Method 1[a] [1/E]	Method 2[b] [Cnst. Flux]	Method 3[c] [BUNKI]	Method 3[c] [BUNKI]	Method 4[d] [In foils]
Total Fluence $[cm^{-2}\ s^{-1}]$	3.68E+03	5.01E+03	5.01E+03	4.78E+03	3.68E+03	3.68E+03
Direct Fluence $[cm^{-2}\ s^{-1}]$	3.58E+03	4.87E+03	4.87E+03	4.64E+03	3.58E+03	3.58E+03
Avg. Energy [MeV]	2.07	2.99	3.35	2.29	2.10	2.2
Direct Dose Equivalent Rate, H_d $[Sv\ h^{-1}]$	0.004290	0.0015854	0.001621	0.006281	0.004075	0.004290
Total Dose Equivalent Rate, $H = H_d + H_s$ $[Sv\ h^{-1}]$	0.004335	0.001602	0.001638	0.006347	0.004119	0.004335
Quality Factor				9.38	9.13	9.92
Error [%]				1.9	3.9	1.2

[a] Method 1 is spectral stripping, flux varies as 1/E within each energy interval.
[b] Method 2 is spectral stripping, constant flux within each energy interval.
[c] Method 3 is spectral unfolding with the BUNKI code.
[d] Method 4 is moderated foil activation (flux integrator & remmeter).

8.2 CONCLUSIONS

The results given in Table 8.1 and the graphs of the spectra indicate that the multisphere system offers the most attractive combination of qualities (measurement of fluence, dose equivalent, and spectral information) of the three neutron detection methods, though the method is not without problems. The larger spheres (10 and 12 inch) are bulky, necessitating a sturdy mounting stand, and precluding their use in less than amply-sized surroundings. Further, unless there is immediate access to TLD readers and a computer workstation for the unfolding code, the method can be time consuming. This is not a problem if immediate results are not required. Finally, as Hertel, et al. [1] have noted, "most Bonner sphere unfolding codes do not yield the true solution or...even a unique solution but one that can be said to be consistent with the input count rates." The solution obtained is dependent upon the initial "guess" input into the code for the neutron fluence, which poses potential pitfalls for the novice unfolding code user.

The moderated foil activation method (flux integrator and remmeter) is also in close agreement with the reference values, but does not provide spectral distribution data. Codes do exist, however, that enable one to unfold spectra obtained from moderated foil data.

The primary problem with the spectral stripping method for the bubble detector spectrometer is that the unfolding is

extremely sensitive to the number of bubbles in each threshold group. If the bubble counts are too low, oscillations in the unfolding imposed by the non-negativity requirement will be a factor that cannot be eliminated without repeating the measurement. BTI recommends that one try to obtain ~3600 bubbles for the 36 BDS detectors, which translates to ~600 bubbles per threshold group, or ~100 bubbles per detector, as a minimum. Improved statistics and better results can be expected if ~1500 bubbles are obtained in each threshold group, although this would necessitate either the use of their BDR-Series II automatic reader, or if manually counting, repeated exposures. The former option is rather expensive, and the latter option could potentially be very time consuming. However, BTI representatives indicate that the main purpose of the BDS is not to obtain a "perfect" spectrum, but rather to provide a rough approximation of the number of neutrons in each threshold or bin [2]. Knowledge of the approximate fluence, combined with the dose equivalent (from the appropriate curves, i.e., ICRP 21) in each bin would provide a truer picture of the neutron dose than is currently available in detectors offering the same degree of portability and ease of use as the BDS system.

BIBLIOGRAPHY

[1] N.E. Hertel, R.S. Hartley, T.L. Bauer, J.L. Horton, and V.A. Otte, "Neutron Measurements in the Vicinity of Medical Electron Accelerators," in Proceedings of the Twentieth Midyear Topical Symposium of the Health Physics Society, Reno, Nevada, CONF-8602106 (1987).

[2] R. Noulty, BTI, 1993 (private communication).

Appendix A

THE BUNKI PROGRAM

The FORTRAN IV program BUNKI was devised by K.A. Lowry and T.L. Johnson at the Naval Research Laboratory to encompass modifications to the SPUNIT or BON31G unfolding codes [1]. BUNKI calculates the fluence, dose, and dose equivalent spectra as a function of neutron energy using the aforementioned codes by utilizing a matrix approximation to solve a degenerate case of a Fredholm integral equation of the first kind. The program also calculates the total fluence, average energy (less thermal), dose, dose equivalent, quality factor, and certain detector responses such as NTA, ANPDR-70, "Hankins" TLD, NRL TLD, and NEUTRAK detectors [2]. Since its inception, BUNKI has evolved into the program utilized in this experiment through minor alterations to include the additional features of spectral plotting via a TOPDRAWER routine [Fermilab] and modification of some arrays to include responses for Chalk River's BDS spectrometry set [SLAC].

BUNKI sessions can be run interactively from a terminal. In an interactive session, BUNKI prompts the user to input options to be used during the session, i.e., type of detector, unfolding code, response matrix, energy intervals, and additional input parameters such as calibration factors, maximum number of iterations, maxwellian temperature, smoothing factor (if any), and error on fitting. Table A.1

provides a description of the input parameters for a BUNKI session.

In lieu of an interactive session, another option for running BUNKI is by means of an executable data file. With this method, one uses an editor such as GNU Emacs, reads the file into Emacs, edits the file's parameters as required, and saves the file back to disk. BUNKI is then executed from the data file. This latter method, rather than the interactive sessions, was employed in the analysis of data from the BDS and multispheres. The data file was called bunin. The bunin file used with the multishpere experimental data for the ^{252}Cf irradiation, with explanations of the parameters, is shown in Table A.2. The items following the double exclamation points are remarks and do not appear in the data file.

The spectrum unfolding output is written directly to disk (user-specified filename). Spectral information written to the file may then be plotted using the TOPDRAWER routine. The BUNKI output file for the multisphere ^{252}Cf irradiation data is presented in Table A.3.

TABLE A.1

Description of Input Parameters of BUNKI[a]

Parameter	Description
SLOPEJ	The initial value of the slope of the 1/E part of the MAXIET spectrum. Usually 0.
PERSLP	The amount by which the slope of the 1/E part of the MAXIET spectrum is changed in searching for a better fit to the data. Typical values, 0.005 - 0.02.
THERMJ	The initial value of the thermal bin of the initial MAXIET spectrum. Usually 0.
THMMIN	The minimum value allowable for the thermal bin of the MAXIET spectrum.
THMMAX	The maximum allowable value for the thermal bin of the MAXIET spectrum. THMMAX and THMMIN are set from physical characteristics of the radiation environment.
DEAD	The dead time of the instrument used to determine the detector counts.
SHP	The minimum value of the (I+1) bin relative to the I bin for the initial MAXIET spectrum. Used to limit the high energy roll-off of the calculated Maxwellian spectrum.
TSTRAT	The maximum allowable value of the error on the fit relative to the value when the error was last tested. Prevents further iterations when no significant improvements in fit is occurring with further iterations. If set > 1.0 this test will not terminate the fit. Typical values: 0.9, 0.99, 0.999, 0.9999, 1.1.
TEMPIJ	The initial guess of the temperature of the Maxwellian peak. Program asks for "Maxwellian Temp." [MeV]
SHAPE	The shape of the high temperature portion of the Maxwellian peak. Typical values, 0-0.5. Originally the program searched for the best shape, but this feature was considered unnecessary and is not user input. Program asks for "shape."
PERTMP	The amount by which the Maxwellian temperature is changed in searching for a better fit to the data. Should be approximately 10% the Maxwellian temperature, TEMPIJ. May be positive, negative, or zero. Positive searches for a lower temperature, negative for a higher temperature. If set to zero, the fit is forced from TEMPIJ which is often a useful feature. Program asks for "perturbation."

Table A.1 (continued)

TSTPER	An end test used to terminate the fit. When the error on the fit drops below this error, the fit is terminated. Program asks for "end test (%)."
SMO	The smoothing factor. Typical values, 0-0.05. Smoothing increases with increasing SMO. Program asks for "smoothing factor."
CAL	A calibration factor used to correct the spectrum to agree with some calibration standard. Typical values found for a 4 mm X 4 mm crystal and the Sanna matrix are 1.2-1.6 for ^{252}Cf. Program asks for "calibration factor."
ITRTST	The number of iterations before making a test to decide if the fit should be terminated. Typical values, 1-100. Program asks for "iterations before error test."
ITRMAX	The maximum number of iterations allowed. Typically 100-1000. May also be set to 0. If the user inputs the initial spectrum and ITRMAX=0, the program does not ask for detector data but calculates the output parameters directly from the input spectrum. This option is useful for calculating integral parameters from known spectra. If using the MAXIET algorithm, setting ITRMAX=0 prevents any further fitting of the data by either SPUNIT or BON31G. The MAXIET spectrum, and calculated integral parameters, are then output in a slightly different format than that shown in Table B.3. Program asks for "maximum number of iterations."
PERTHM	The amount by which the thermal bin of the MAXIET spectrum is changed in searching for a better fit to the data. PERTHM is not input directly, but is calculated from PERSLP.
PERE	The amount by which the magnitude of the 1/E part of the MAXIET spectrum is changed in searching for a better fit to the data. PERE is not input directly, but is calculated from PERSLP. A reasonable relationship between PERSLP, PERTHM, and PERE must be maintained to insure that the MAXIET algorithm will find the best fit to the detector data.

[a]From NRL Memorandum Report 5340, Appendix B.

TABLE A.2

Sample Bunin File

File Contents	Explanation
31	!! # of groups
6	!! # of detectors
2	!! code for det #1
3	!! code for det #2
5	!! code for det #3
8	!! code for det #4
10	!! code for det #5
12	!! code for det #6
SAN13	!! response matrix
SPUNIT	!! unfolding algorithm
Y	!! put spectra in file for plotting?
1	!! file # of the spectrum
252Cf TLD/Bonner Sphere Unfolding Experiment Date:24Mar93	!! heading for output
Y	!! search for maxwell, 1/E init. spectrum?
1.05, 0.0, 0.0	!! maxwellian temp., shape, perturbation
1.0, 0.0, 1.096e7, 10, 750	!! end test [%], smooth.fac., calib.fac., err.it, max.iter.
0.166, 8.00	!! sphere count, error [%]
0.654, 6.00	!! sphere count, error [%]
1.848, 3.00	!! sphere count, error [%]
1.850, 3.00	!! sphere count, error [%]
1.270, 4.00	!! sphere count, error [%]
0.961, 5.00	!! sphere count, error [%]
Y	!! save results?
Y	!! last spectrum (is this)?
N	!! louhi data (y or no)

TABLE A.3

Sample BUNKI Output File

252Cf TLD/Bonner Sphere Unfolding Experiment Date: 24-25 Mar 93 SAN13

RESPONSE MATRIX	UNFOLD CODE	MAXWELL TEMP,SHAPE	CALIB. FACTOR	SMOOTH FACTOR	PER CENT ERROR	NO. OF ITERATIONS
SAN13	SPUN	1.05, .00	******	.0000	3.8973	750

DETECTORS	MEASURED COUNTS	CALCULATED COUNTS	PERCENT DIFFERENCE
2 INCH OR BDS-600	.166	.168	1.418
3 INCH OR BDS-2500	.654	.653	-.148
5 INCH	1.848	1.777	-3.847
8 INCH	1.850	1.845	-.256
10 INCH	1.270	1.363	7.342
12 INCH	.961	.918	-4.509

TOTAL FLUENCE=	1.287E+07	NEUTRONS/CM2
AVE ENERGY (LESS TH)=	2.103E+00	MEV
DOSE=	4.463E-02	RAD
DOSE EQUIVALENT=	4.075E-01	REM
QUALITY FACTOR=	9.129	REM/RAD
NRL TLD RESPONSE=	1.022	REM/REM(CF-252)
"HANKINS" TLD RESPONSE=	1.093	REM/REM(CF-252)
NEUTRAK RESPONSE=	.938	REM/REM(CF-252)
NTA RESPONSE=	.959	REM/REM(CF-252)
ANPDR-70 RESPONSE=	.972	REM/REM(CF-252)

BIN NO.	ENERGY MAX (MEV)	FLUENCE NEUT/CM2	FLUENCE N/CM2/LETH	DOSE (RAD)	DOSE EQV. (REM)	DOSE EQV. (% OF TOTAL)
1	4.140E-07	4.418E-03	2.732E-03	2.324E-12	5.085E-12	1.248E-09
2	6.826E-07	1.050E-02	4.835E-02	6.392E-12	1.294E-11	3.175E-09
3	1.445E-06	2.623E-02	8.054E-02	1.620E-11	3.290E-11	8.073E-09
4	3.059E-06	5.169E-02	1.587E-01	3.171E-11	6.430E-11	1.578E-08
5	6.476E-06	1.045E-01	3.207E-01	6.341E-11	1.282E-10	3.146E-08
6	1.371E-05	2.175E-01	6.677E-01	1.307E-10	2.634E-10	6.464E-08
7	2.902E-05	4.669E-01	1.434E+00	2.788E-10	5.580E-10	1.369E-07
8	6.144E-05	1.033E+00	3.171E+00	6.133E-10	1.218E-09	2.989E-07
9	1.301E-04	2.377E+00	7.7294+00	1.400E-09	2.759E-09	6.772E-07
10	2.754E-4	5.631E+00	1.729E+01	3.208E-09	6.323E-09	1.552E-06
11	5.929E-04	1.404E+01	4.217E+01	7.675E-09	1.517E-08	3.722E-06
12	1.234E-03	3.419E+01	1.074E+02	1.795E-08	3.556E-08	8.726E-06
13	2.613E-03	9.018E+01	2.768E+02	4.643E-08	9.198E-08	2.257E-05
14	5.531E-03	2.448E+02	7.516E+02	1.244E-07	2.467E-07	6.055E-05
15	1.171E-02	7.013E+02	2.153E+03	3.534E-07	7.076E-07	1.737E-04
16	2.479E-02	2.206E+03	6.773E+03	1.242E-06	3.340E-06	8.197E-04
17	5.247E-02	8.151E+03	2.503E+04	5.411E-06	2.190E-05	5.375E-03
18	1.111E-01	3.920E+04	1.203E+05	3.076E-05	1.872E-04	4.594E-02
19	2.237E-01	2.149E+05	7.069E+05	2.230E-04	1.783E-03	4.376E-01
20	4.508E-01	1.042E+06	3.423E+06	1.151E-03	1.475E-02	3.620E+00
21	9.072E-01	3.517E+06	1.158E+07	7.892E-03	8.409E-02	2.064E+01
22	1.872E+00	3.441E+06	1.094E+07	1.172E-02	1.207E-01	2.961E+01
23	3.679E+00	2.390E+06	8.144E+06	1.008E-02	9.547E-02	2.343E+01
24	7.408E+00	1.825E+06	6.005E+06	1.055E-02	7.433E-02	1.824E+01
25	1.492E+01	3.886E+05	1.278E+06	2.573E-03	1.597E-02	3.920E+00
26	2.581E+01	4.358E+03	1.831E+04	3.964E-05	1.898E-04	4.659E-02
27	4.465E+01	6.671E+01	2.803E+02	6.411E-07	2.955E-06	7.253E-04
28	7.725E+01	9.989E-01	4.196E+00	1.012E-08	4.707E-08	1.155E-05
29	1.336E+02	1.412E-02	5.935E-02	1.606E-10	7.097E-10	1.742E-07
30	2.312E+02	1.861E-04	7.814E-04	2.773E-12	1.030E-11	2.529E-09
31	4.000E+02	2.081E-06	8.743E-06	3.734E-14	1.323E-13	3.248E-11

BIBLIOGRAPHY

[1] Lowry, K. A. and Johnson, T.L., "Modifications to Iterative Recursion Unfolding Algorithms and Computer Codes to Find More Appropriate Neutron Spectra," Naval Research Laboratory, Washington, D.C., NRL Memorandum Report 5340 (1984).

[2] Computer program BUNKI03 (Naval Research Laboratories, Washington, D.C., 1983).

APPENDIX B

PuBe Calculations

Appendix B contains the worksheets used in calculating the dosimetric parameters of the ^{238}PuBe source on the dates of March 11, 1993, and June 2, 1993, as well as one of the worksheets used to calculate the approximate irradiation times for at least 70 bubbles per bubble detector.

The BUNKI output file from V. Vylet of SLAC for the same PuBe source obtained with Bonner Multispheres and a source-to-detector-distance of 80 cm is given below.

BIN NO.	ENERGY MAX (MEV)	FLUENCE NEUT/CM2	FLUENCE N/CM2/LETH	DOSE (RAD)	DOSE EQV. (REM)	DOSE EQV. (% OF TOTAL)
1	4.140E-07	9.530E-05	5.894E-05	5.013E-14	1.097E-13	5.021E-10
2	6.826E-07	5.648E-05	2.601E-04	3.439E-14	6.959E-14	3.185E-10
3	1.445E-06	9.103E-05	2.795E-04	5.621E-14	1.142E-13	5.225E-10
4	3.059E-06	1.040E-04	3.192E-04	6.378E-14	1.293E-13	5.920E-10
5	6.476E-06	1.337E-04	4.103E-04	8.113E-14	1.640E-13	7.507E-10
6	1.371E-05	2.182E-04	6.699E-04	1.311E-13	2.643E-13	1.210E-09
7	2.902E-05	7.136E-04	2.191E-03	4.260E-13	8.527E-13	3.903E-09
8	6.144E-05	2.344E-03	7.195E-03	1.391E-12	2.763E-12	1.265E-08
9	1.301E-04	7.740E-03	2.376E-02	4.561E-12	8.987E-12	4.113E-08
10	2.754E-04	2.565E-02	7.877E-02	1.462E-11	2.881E-11	1.319E-07
11	5.929E-04	8.728E-02	2.621E-01	4.770E-11	9.426E-11	4.314E-07
12	1.234E-03	2.860E-01	8.985E-01	1.502E-10	2.975E-10	1.362E-06
13	2.613E-03	9.574E-01	2.938E+00	4.929E-10	9.765E-10	4.470E-06
14	5.531E-03	3.229E+00	9.916E+00	1.641E-09	3.255E-09	1.490E-05
15	1.171E-02	1.096E+01	3.365E+01	5.523E-09	1.106E-08	5.062E-05
16	2.479E-02	3.755E+01	1.153E+02	2.114E-08	5.685E-08	2.602E-04
17	5.247E-02	1.309E+02	4.019E+02	8.688E-08	3.516E-07	1.609E-03
18	1.111E-01	4.701E+02	1.443E+03	3.689E-07	2.245E-06	1.028E-02
19	2.237E-01	1.620E+03	5.331E+03	1.682E-06	1.345E-05	6.155E-02
20	4.508E-01	5.627E+03	1.849E+04	8.181E-06	7.967E-05	3.647E-01
21	9.072E-01	2.152E+04	7.084E+04	4.828E-05	5.145E-04	2.355E+00
22	1.872E+00	8.429E+04	2.679E+05	2.871E-04	2.955E-03	1.353E+01
23	3.679E+00	1.946E+05	6.631E+05	8.210E-04	7.773E-03	3.558E+01
24	7.408E+00	2.161E+05	7.110E+05	1.249E-03	8.800E-03	4.028E+01
25	1.492E+01	4.120E+04	1.355E+05	2.728E-04	1.694E-03	7.753E+00
26	2.581E+01	3.413E+02	1.434E+03	3.105E-06	1.487E-05	6.805E-02
27	4.465E+01	3.743E+00	1.573E+01	3.597E-08	1.658E-07	7.591E-04
28	7.725E+01	4.013E-02	1.686E-01	4.065E-10	1.891E-09	8.656E-06
29	1.336E+02	4.182E-04	1.758E-03	4.755E-12	2.102E-11	9.621E-08
30	2.312E+02	4.277E-06	1.795E-05	6.372E-14	2.367E-13	1.084E-09
31	4.000E+02	4.021E-08	1.689E-07	7.214E-16	2.557E-15	1.170E-11

Worksheet: Characterization of the Radioisotopic ^{238}PuBe Neutron Source
Source ID is MRC–426 (Monsanto Research Corporation)

^{238}Pu $T_{1/2}$= 87.74 yr Average Energy = 4.2 MeV

Neutron emission rate
as of 5/1/90 = 1.84E+07 s^{-1}, +/– 10%

Elapsed time as of 03/11/93 = 1045 days = 2.861054 yr.

Neutron emission rate
as of 03/11/93 = 1.799E+07 s^{-1}, +/– 10% MRC 426

Direct Fluence Rate (phi_d) = NF/4 pi r^2 where N = neutron emission rate
F = anisotropic factor = 1.09, from SLAC–TN–91–3, Oct. 91
r = source–to–detector distance in cm

Source–to–detector distance (r)= 50 cm
Height for source (h) = 160 cm

phi_d
as of 03/11/93 = 624 n/cm^2s MRC 426

Scattered/direct fluence ratio (f_{phi} =phi_s/phi_d) estimated from Schwarz's formula:

$f_{phi} = 2.16hr^2r_i^{-3}$ where r_i = Image source–to–detector distance
r_i = SQRT{$r^2 + (2h)^2$} with r, h, in cm

r_i = 323.88 cm

f_{phi} = 2.54% @ r = 50 cm
2.54% using Jenkins' recipe

Total fluence rate $phi_{total} = phi_d + phi_s$ = 640.0 n/cm^2s MRC 426

Direct Dose Equiv. Rate
(H_d) as of 5/1/90 = 83.6 mrem/hr @ 0.5 m (+/– 10%)
20.9 mrem/hr @ 1 m (+/– 10%)

(H_d) as of 03/11/93 = 81.93 mrem/hr @ 0.5 m 0.444444 0.75 cm factor
36.41 mrem/hr @ 0.75 m
20.43 mrem/hr @ 1 m

Scattered/direct dose equivlalent ratio ($f_H = H_s/H_d$) estimated from Schwarz's formula:

$f_H = 0.8hr^2r_i^{-3}$ = 0.94% @ r = 50 cm
1.78% using Jenkins' recipe

Total Dose Equiv. Rate
($H_{total} = H_d + H_s$)

as of 03/11/93 =		Jenkins'
	82.70 mrem/hr @ 0.5 m	83.39 mrem/hr @ 0.5 m
	36.75 mrem/hr @ 0.75 m	37.06 mrem/hr @ 0.75 m
	20.63 mrem/hr @ 1 m	20.80 mrem/hr @ 1 m

Worksheet: Characterization of the Radioisotopic ^{238}PuBe Neutron Source
Source ID is MRC–426 (Monsanto Research Corporation)

^{238}Pu $T_{1/2}$= 87.74 yr Average Energy = 4.2 MeV

Neutron emission rate
as of 5/1/90 = 1.84E+07 s^{-1}, +/– 10%

Elapsed time as of 06/02/93 = 1128 days = 3.088296 yr.

Neutron emission rate
as of 06/02/93 = 1.796E+07 s^{-1}, +/– 10%

Direct Fluence Rate (phi_d) = NF/4 pi r^2 where N = neutron emission rate
F = anisotropic factor = 1.09, from SLAC–TN–91–3, Oct. 91
r = source–to–detector distance in cm

Source–to–detector distance (r)= 50 cm
Height for source (h) = 160.6 cm

phi_d
as of 06/02/93 = 623 n/cm^2s

Scattered/direct fluence ratio (f_{phi} =phi_s/phi_d) estimated from Schwarz's formula:

$f_{phi} = 2.16hr^2r_i^{-3}$ where r_i = Image source–to–detector distance
r_i = SQRT{$r^2 + (2h)^2$} with r, h, in cm

r_i = 325.07 cm

f_{phi} = 2.52% @ r = 50 cm
2.52% using Jenkins' recipe

Total fluence rate $phi_{total} = phi_d + phi_s$ = 638.7 n/cm^2s

Direct Dose Equiv. Rate
(H_d) as of 5/1/90 = 83.8 mrem/hr @ 0.5 m (+/– 10%)
20.9 mrem/hr @ 1.0 m (+/– 10%)

(H_d) as of 06/02/93 = 81.78 mrem/hr @ 0.5 m 0.444444 0.75 cm factor
36.35 mrem/hr @ 0.75 m
20.40 mrem/hr @ 1 m

Scattered/direct dose equivlalent ratio ($f_H = H_s/H_d$) estimated from Schwarz's formula:

$f_H = 0.8hr^2r_i^{-3}$ = 0.94% @ r = 50 cm
1.77% using Jenkins' recipe

Total Dose Equiv. Rate
($H_{total} = H_d + H_s$)

as of 06/02/93 =		Jenkins'
	82.55 mrem/hr @ 0.5 m	83.23 mrem/hr @ 0.5 m
	36.69 mrem/hr @ 0.75 m	36.99 mrem/hr @ 0.75 m
	20.59 mrem/hr @ 1 m	20.76 mrem/hr @ 1 m

Worksheet: Approximate Irradiation Times for at Least 70 Bubbles per Detector
Temperature assumed to be 20 C
^{238}PuBe Source as of May 20, 1993

Direct Dose Equivalent rate = 81.80 mrem/hour
= 1.36 mrem/min
= 0.023 mrem/sec

Detector Threshold	S/N (414 prfx)	Sensitivity Bub/mrem	Bubbles per min.	Time for 70 Bub.	Average Minutes
BDS−10	15	0.51	0.695	100.68 minutes	
	16	0.52	0.709	98.74	
	17	0.55	0.750	93.35	
	18	0.55	0.750	93.35	
	19	0.62	0.845	82.81	
	20	0.64	0.873	80.23	92
BDS−100	21	0.92	1.254	55.81 minutes	
	22	0.96	1.309	53.48	
	23	1.2	1.636	42.79	
	24	1.3	1.772	39.50	
	25	1.3	1.772	39.50	
	26	1.3	1.772	39.50	45
BDS−600	27	1.9	2.590	27.02 minutes	
	28	1.9	2.590	27.02	
	29	2	2.727	25.67	
	30	2.7	3.681	19.02	
	31	2.7	3.681	19.02	
	32	2.8	3.817	18.34	23
BDS−100(	33	3.8	5.181	13.51 minutes	
	34	3.9	5.317	13.17	
	35	3.9	5.317	13.17	
	36	3.9	5.317	13.17	
	37	4.2	5.726	12.22	
	38	4.2	5.726	12.22	13
BDS−250(	39	5.5	7.498	9.34 minutes	
	40	5.5	7.498	9.34	
	41	5.6	7.635	9.17	
	42	5.6	7.635	9.17	
	43	5.8	7.907	8.85	
	44	6.1	8.316	8.42	9
BDS−10K	45	0.55	0.750	93.35 minutes	
	46	0.57	0.777	90.08	
	47	0.59	0.804	87.02	
	48	0.61	0.832	84.17	
	49	0.61	0.832	84.17	
	50	0.61	0.832	84.17	87

Appendix C

CALCULATION OF THE FLUENCE-TO-DOSE-EQUIVALENT CONVERSION FACTOR (FDECF) FOR THE BUBBLE DETECTOR SPECTROMETER (BDS)

METHOD 1: Assumption of Constant Fluence per Unit Energy within Each Energy Interval

Energy Interval [1]	FDECF (10^{-10} Sv cm^2) [2]
0.025 - 0.4 eV	$h_\Phi(E) := 0.11$
0.4 eV - 10 keV	$h_\Phi(E) := 0.102$
10 keV - 1 MeV	$h_\Phi(E) := 0.01679 \cdot E^{0.7673}$
1 - 2 MeV	$h_\Phi(E) := 0.5097 \cdot E^{0.2706}$
2 - 10 MeV	$h_\Phi(E) := 4.06$

NOTE: E is neutron energy in keV.

(For this calculation, the arbitrary value of 5000 has been assigned for the flux.)

Energy intervals for BDS System (in keV)

Interval 1:	10 - 100 keV	Interval 4:	1000 - 2500 keV
Interval 2:	100 - 600 keV	Interval 5:	2500 - 10000 keV
Interval 3:	600 - 1000 keV	Interval 6:	10000 - 20000 keV

Calculation of coefficients for interval 6 and interval 5

$h_{\Phi 6}(E) := 4.06$ $\quad \Phi(E) := 5000$ $\quad h_{\Phi 5}(E) := 4.06$

$$\frac{\int_{2500}^{10000} h_{\Phi 6}(E)\cdot\Phi(E)\,dE}{\int_{2500}^{10000} \Phi(E)\,dE} = 4.06$$

$$\frac{\int_{10000}^{20000} h_{\Phi 5}(E)\cdot\Phi(E)\,dE}{\int_{10000}^{20000} \Phi(E)\,dE} = 4.06$$

METHOD 1: Assumption of Constant Fluence (continued)

Calculation of coefficient for Interval 4

$$h_{\Phi 4}(E) := 0.5097 \cdot E^{.2706} \qquad h_{\Phi 5}(E) := 4.06$$

$$\frac{\int_{1000}^{2000} h_{\Phi 4}(E)\cdot\Phi(E)\,dE + \int_{2000}^{2500} h_{\Phi 5}(E)\cdot\Phi(E)\,dE}{\int_{1000}^{2500} \Phi(E)\,dE} = 3.803$$

Calculation of coefficient for Interval 3

$$h_{\Phi 3}(E) := 0.01679 \cdot E^{.7673}$$

$$\frac{\int_{600}^{1000} h_{\Phi 3}(E)\cdot\Phi(E)\,dE}{\int_{600}^{1000} \Phi(E)\,dE} = 2.83$$

Calculation of coefficient for Interval 2

$$h_{\Phi 2}(E) := 0.01679 \cdot E^{0.7673}$$

$$\frac{\int_{100}^{600} h_{\Phi 2}(E)\cdot\Phi(E)\,dE}{\int_{100}^{600} \Phi(E)\,dE} = 1.479$$

Calculation of coefficient for Interval 1

$$h_{\Phi 1}(E) := 0.01679 \cdot E^{0.7673}$$

$$\frac{\int_{10}^{100} h_{\Phi 1}(E)\cdot\Phi(E)\,dE}{\int_{10}^{100} \Phi(E)\,dE} = 0.355$$

In Table Form:

BDS Interval		Coefficient (10^{-10} Sv cm^2)
Interval 1:	10 - 100 keV	$h_{\Phi 1} := 0.355$
Interval 2:	100 - 600 keV	$h_{\Phi 2} := 1.479$
Interval 3:	600 - 1000 keV	$h_{\Phi 3} := 2.83$
Interval 4:	1000 - 2500 keV	$h_{\Phi 4} := 3.803$
Interval 5:	2500 - 10000 keV	$h_{\Phi 5} := 4.06$
Interval 6:	10000 - 20000 keV	$h_{\Phi 6} := 4.06$

METHOD 2: Assumption that Fluence Varies as 1/E within Each Energy Interval

Energy Interval [1]	FDECF (10^{-10} Sv cm^2)
0.025 - 0.4 eV	$h_\Phi(E) := 0.11$
0.4 eV - 10 keV	$h_\Phi(E) := 0.102$
10 keV - 1 MeV	$h_\Phi(E) := 0.01679 \cdot E^{0.7673}$
1 - 2 MeV	$h_\Phi(E) := 0.5097 \cdot E^{0.2706}$
2 - 10 MeV	$h_\Phi(E) := 4.06$

NOTE: E is neutron energy in keV.

Energy intervals for BDS System (in keV)

Interval 1:	10 - 100 keV	Interval 4:	1000 - 2500 keV
Interval 2:	100 - 600 keV	Interval 5:	2500 - 10000 keV
Interval 3:	600 - 1000 keV	Interval 6:	10000 - 20000 keV

Calculation of coefficients for Interval 6 and Interval 5

$h_{\Phi 6}(E) := 4.06$ $\quad \Phi(E) := \frac{1}{E}$ $\quad h_{\Phi 5}(E) := 4.06$

$$\frac{\int_{2500}^{10000} h_{\Phi 6}(E)\cdot\Phi(E)\,dE}{\int_{2500}^{10000} \Phi(E)\,dE} = 4.06 \qquad \frac{\int_{10000}^{20000} h_{\Phi 5}(E)\cdot\Phi(E)\,dE}{\int_{10000}^{20000} \Phi(E)\,dE} = 4.06$$

Calculation of coefficient for Interval 4

$h_{\Phi 4}(E) := 0.5097 \cdot E^{.2706}$ $\quad h_{\Phi 5}(E) := 4.06$

$$\frac{\int_{1000}^{2000} h_{\Phi 4}(E)\cdot\Phi(E)\,dE \div \int_{2000}^{2500} h_{\Phi 5}(E)\cdot\Phi(E)\,dE}{\int_{1000}^{2500} \Phi(E)\,dE} = 3.738$$

METHOD 2: Assumption that Fluence Varies as 1/E (continued)

Calculation of coefficient for Interval 3

$$h_{\Phi 3}(E) := 0.01679 \cdot E^{.7673}$$

$$\frac{\int_{600}^{1000} h_{\Phi 3}(E) \cdot \Phi(E)\, dE}{\int_{600}^{1000} \Phi(E)\, dE} = 2.784$$

Calculation of coefficient for Interval 2

$$h_{\Phi 2}(E) := 0.01679 \cdot E^{0.7673}$$

$$\frac{\int_{100}^{600} h_{\Phi 2}(E) \cdot \Phi(E)\, dE}{\int_{100}^{600} \Phi(E)\, dE} = 1.236$$

Calculation of coefficient for Interval 1

$$h_{\Phi 1}(E) := 0.01679 \cdot E^{0.7673}$$

$$\frac{\int_{10}^{100} h_{\Phi 1}(E) \cdot \Phi(E)\, dE}{\int_{10}^{100} \Phi(E)\, dE} = 0.27$$

In Table Form:

BDS Interval		Coefficient (10^{-10} Sv cm^2)
Interval 1:	10 - 100 keV	$h_{\Phi 1} := 0.27$
Interval 2:	100 - 600 keV	$h_{\Phi 2} := 1.236$
Interval 3:	600 - 1000 keV	$h_{\Phi 3} := 2.784$
Interval 4:	1000 - 2500 keV	$h_{\Phi 4} := 3.738$
Interval 5:	2500 - 10000 keV	$h_{\Phi 5} := 4.06$
Interval 6:	10000 - 20000 keV	$h_{\Phi 6} := 4.06$

BIBLIOGRAPHY

[1] J.C. Liu, C.S. Sims, and J.W. Poston, "The Development, Characterization, and performance Evaluation of a New Combination Type Personnel Neutron Dosimeter," ORNL-6593 (Oct. 1989).

[2] International Commission on Radiological Protection, "Data for Protection against Ionizing Radiation from External Sources," ICRP Report No. 21 (1971).

Appendix D

DECONVOLUTION OF SPECTRAL DATA FOR THE BUBBLE DETECTOR SPECTROMETER

One of the rudimentary methods used in this study to unfold the spectral data obtained from the BDS is termed "spectral stripping." The method allows one to manually calculate the neutron spectrum (as opposed to the use of more sophisticated computer unfolding codes), but it is well known to suffer from error accumulation as the stripping continues. Unfortunately, this accumulation of error will ultimately affect the quality of the unfolded spectral result, particularly with regard to the lower energy region of the spectrum since the method begins with the high energy end of the spectrum and continues downward. In the BDS manual, it is stated that certain assumptions must be made when using the spectral stripping method, which are [1]:

1. The derived unfolded spectrum can be adequately approximated by a six region histogram (six threshold detectors).
2. Neutrons detected by the BDS-10000 range between 10 and 20 MeV. This is a reasonable assumption as most dosimetric interest lies below 20 MeV.
3. Fluence per unit energy is constant over the histogram interval.

The spectral stripping calculations were performed in the following manner:

A. Following irradiation and an appropriate waiting period (approximately 30 minutes) to allow the bubbles to grow large enough for visual counting, the number of bubbles in each detector was counted. This number was recorded as A_i.

B. Each A_i was normalized to a detector of unit sensitivity via division of A_i by the individual detector's sensitivity provided by BTI in the shipping data sheet.

$$A_i/\text{sensitivity} = R_i$$

Thus, R_i is the standardized response. The subscript i corresponds with the energy threshold of the detectors in the BDS. For the BDS-10, i = 1, for the BDS-100, i = 2, and so on, up to i = 6 for the BDS-10000.

C. As six detectors of identical threshold energies (group) were irradiated simultaneously, an average R_i was calculated for the group. This was done for all six groups, hence R_1 = the standardized response of the six BDS-10s, continuing up to R_6 = the standardized response of the six BDS-10000s.

D. Table D.1 provides the average cross sections for the BDS over various energy ranges in the format σ_{ij}, where i is the same as in step **B** above and j = the histogram interval index from 1 to 6. Using the appropriate σ_{ij} from Table D.1, the number of neutrons in the corresponding histogram N_i was calculated, beginning with R_6, as follows:

$$R_6 = (\sigma_{66})(N_6) \qquad (1)$$

where σ_{66} is the average response of the BDS-10000 detectors over

the interval 10-20 MeV (e.g., 4.35 X 10^{-5} from Table D.1), R_6 is the averaged standardized response of the BDS-10000 from step **C**, and N_6 is the total neutron fluence over the interval from 10 to 20 MeV. After determining N_6, the fluence of the next histogram (N_5) was calculated using

$$R_5 = (\sigma_{55})(N_5) + (\sigma_{56})(N_6) \qquad (2)$$

where σ_{55} is the average response of the BDS-2500 detectors over the interval 2.5 to 10 MeV, σ_{56} is the average response of the BDS-2500 detectors over the interval 10 to 20 MeV, and N_6 was calculated in equation (1). This procedure was continued until all of the neutron fluences N_i in each of the six histograms were obtained.[1]

E. The fluence per MeV in each histogram is found by

$$N_i/\Delta E_i$$

where ΔE_i is the bin width of the respective histogram in MeV.

F. The total fluence ϕ over the exposure time of the detectors is given by

$$\phi = \sum_{i=1}^{6} N_i$$

---

[1] There is a "non-negativity" condition imposed on the spectral stripping method. In some histogram intervals, there may be very few or no neutrons in the source spectrum. Due to statistical uncertainly, the value of N_i may be negative in these intervals. In instances where this was the case, the respective N_i was replaced by zero.

TABLE D.1

Average Cross Sections of BDS over Various Energy Ranges

Detector I.D.	j=	HISTOGRAM INTERVAL 1 (0.01-0.1)	2 (0.1-0.6)	3 (0.6-1.0)	4 (1.0-2.5)	5 (2.5-10)	6 (10-20) MeV
BDS-10	1	5.00E-06	2.50E-05	2.92E-05	2.97E-05	4.15E-05	4.78E-05
BDS-100	2	-	2.27E-05	3.14E-05	3.23E-05	4.47E-05	5.09E-05
BDS-600	3	-	-	1.60E-05	3.27E-05	4.75E-05	5.45E-05
BDS-1000	4	-	-	-	1.32E-05	3.50E-05	5.90E-05
BDS-2500	5	-	-	-	-	2.99E-05	8.70E-05
BDS-10000	6	-	-	-	-	-	4.35E-05

BIBLIOGRAPHY

[1] Bubble Technology Industries "Instruction Manual for the Bubble Detector Spectrometer (BDS)," BTI, Inc., January 31, 1992.

Appendix E

CALCULATION OF THE AVERAGE NEUTRON ENERGY FOR THE SPECTRAL STRIPPING METHOD

Method 1: Assumption of Constant E

The definition of average energy is given by:

$$\bar{E} \equiv \frac{\int_0^\infty \phi(E)\, E\, dE}{\int_0^\infty \phi(E)\, dE} \qquad \text{where } \phi(E) = \phi_i/\Delta E_i, \quad i = 1, 2, \ldots 6$$

The energy intervals are:

E_1	=	0.01	MeV
E_2	=	0.1	MeV
E_3	=	0.6	MeV
E_4	=	1.0	MeV
E_5	=	2.5	MeV
E_6	=	10	MeV
E_{max}	=	20	MeV

The expression is then given by

$$\bar{E} = \frac{\int_1^2 \phi_1(E)\, E\, dE + \int_2^3 \phi_2(E)\, E\, dE + \ldots \int_5^6 \phi_6(E)\, E\, dE}{\sum_{i=1}^{6} \phi_i}$$

Substituting the expression for $\phi(E)$ given above, we have

$$\bar{E} = \frac{(\phi_1/\Delta E_1)\int_{E_1}^{E_2} E\, dE + (\phi_2/\Delta E_2)\int_{E_2}^{E_3} E\, dE + \ldots (\phi_6/\Delta E_6)\int_{E_6}^{E_{max}} E\, dE}{\sum_{i=1}^{6} \phi_i}$$

where

$$\phi_1(E) = \phi_1/(E_2 - E_1),\ \phi_2(E) = \phi_2/(E_3 - E_2) \ldots \phi_6(E) = \phi_6/(E_{max} - E_6)$$

Method 2: 1/E Assumption

In this case, $\phi_i(E) = C/E$ where C is some constant over the interval, and i = 1, 2, 3,...6, and the energy intervals are the same as in Method 1. Hence we have

$$\bar{E} \equiv \frac{\int_{E_0}^{E_1} \phi(E)\ E\ dE}{\sum_{i=1}^{6} \phi_i} = \frac{C_1 \int_{E_i}^{E_{i+1}} (C_i/E_i) E_i\ dE}{\sum_{i=1}^{6} \phi_i}$$

Evaluating $\phi_1 = \int C/E\ dE$ yields

$$C_1 = \phi_1 / \ln(E_2/E_1)$$

which is substituted into the expression to give

$$\bar{E} = \frac{\sum_{i=1}^{6} \phi i / \ln(Ei+1/Ei) \int_{E_i}^{E_{i+1}} dE}{\sum_{i=1}^{6} \phi_i} = \frac{\sum \phi_i (E_{i+1} - E_i) / \ln(E_{i+1}/E_i)}{\sum_{i=1}^{6} \phi_i} \quad \text{in MeV}$$